NOAA Technical Memorandum ERL PMEL-44

MARINE WEATHER OF THE INLAND WATERS OF WESTERN WASHINGTON

James E. Overland
Bernard A. Walter, Jr.

Pacific Marine Environmental Laboratory
Seattle, Washington
January 1983

UNITED STATES
DEPARTMENT OF COMMERCE
Malcolm Baldrige,
Secretary

NATIONAL OCEANIC AND
ATMOSPHERIC ADMINISTRATION
John V. Byrne,
Administrator

Environmental Research
Laboratories
George H. Ludwig
Director

CONTENTS

Figures

Tables

Marine Weather of the Inland Waters of Western Washington[1]

James E. Overland and Bernard A. Walter, Jr.

ABSTRACT. The mid-latitude, west coast marine climate of western Washington is typified in summer by high sea-level pressure as part of the North Pacific weather pattern and in winter by a sequence of storms which originate to the west. Mean and extreme temperatures are moderated by the proximity of the Pacific Ocean and Puget Sound, resulting in an mean temperature of 4°C in January and 17°C in August at Seattle.

Local variations in precipitation and wind are influenced by both large-scale weather patterns and the region's topography. Fifty percent of the annual precipitation for most of the inland region falls in the four months from November through February, and less than five percent falls in July and August; the driest region is to the northeast of the Olympic Mountains. Over the inland waters, the winds flow from high to low sea-level pressure in the direction of the local channels.

Recent studies by the University of Washington and PMEL on the Puget Sound convergence zone, sea and valley breeze, precipitation patterns and local wind patterns are summarized. The storm which resulted in destruction of the Hood Canal Bridge has shown that the presence of the Olympic Mountains can induce a regional low-pressure system in their lee which can result in strong surface winds over the inland waters.

---

[1]Contribution number 595 from the NOAA/ERL Pacific Marine Environmental Laboratory, 3711 15th Avenue N.E., Seattle, Washington 98105.

1. Introduction

The climate of the Puget Sound Basin in western Washington State is a mid-latitude, west coast marine type. The source regions of the predominant air masses reaching Puget Sound are over the Pacific Ocean; this produces a moderating influence on the weather in both summer and winter. A prevailing westerly-to-northwesterly flow of air associated with high sea-level pressure in the eastern Pacific results in a dry season beginning in June and reaching a peak in midsummer.[1] In the late fall and winter the high-pressure area retreats to the south allowing a series of storms to cross the region, thus effecting a wet season that begins in October, reaches a peak in winter, and decreases in the spring. This winter pattern is occasionally interrupted by the influence of continental high pressure which is accompanied by cold temperatures and dry air.

Topography has a large influence on the weather of Puget Sound (Figs. 1 and 2). The region is flanked on the west by the Olympic Mountains and on the east by the Cascade Range. The elevation of the region varies from sea level on the Sound to 2500 m and higher in the mountains. The Cascades and the Canadian Rocky Mountains shield Puget Sound from cold air masses moving southward across Canada. To the west, the Willapa Hills (which lie south of Hoquiam, Washington), the Olympic Mountains, and the Coastal Range on Vancouver Island are effective in protecting the area from more intense winter storms that reach the coast by forcing orographic precipitation on the western slopes (Hobbs et al., 1975). The Strait of Juan de Fuca, the Strait of Georgia, and the Chehalis River Valley provide low-level passages for maritime air to move inland and are the primary determinant of surface winds.

The next section provides a climatological overview of air temperature, precipitation, winds, and other important climatological variables for the Puget Sound Basin. Section 3 discusses the synoptic or large-scale distribution and propagation of high and low sea-level pressure patterns that influence the meteorology of western Washington. Section 4 provides a summary of a number of regional meteorological phenomena that contribute to the climatology of the region.

2. Climatological Summary

2.1. Air temperature

The yearly cycle and variability of monthly mean temperatures measured at SEATAC Airport, 20 miles south of Seattle, are shown in Fig. 3. During the

[1]The meteorological convention of specifying the direction from which the wind is blowing is used throughout this memorandum.

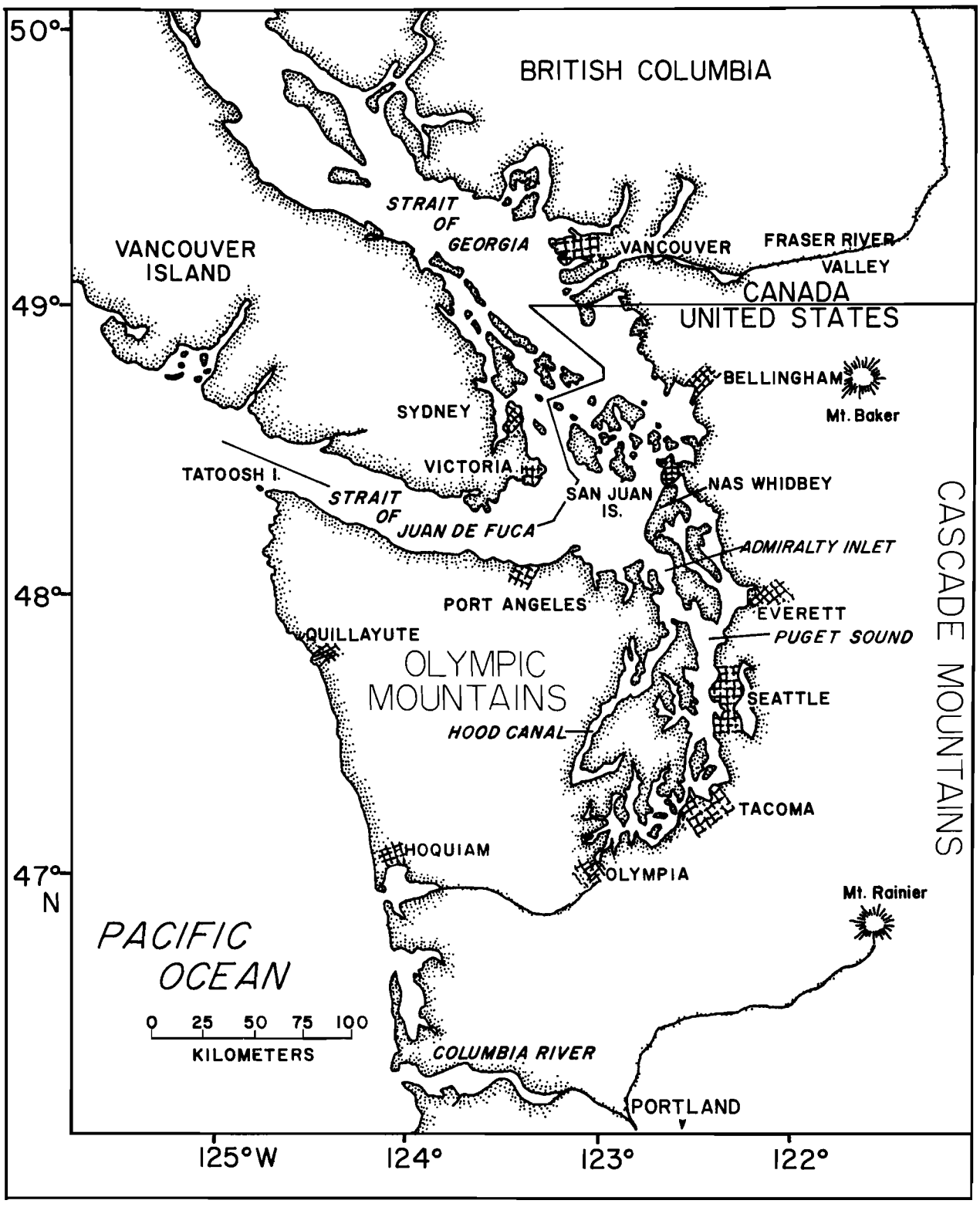

Figure 1. Location map for western Washington and southwest British Columbia.

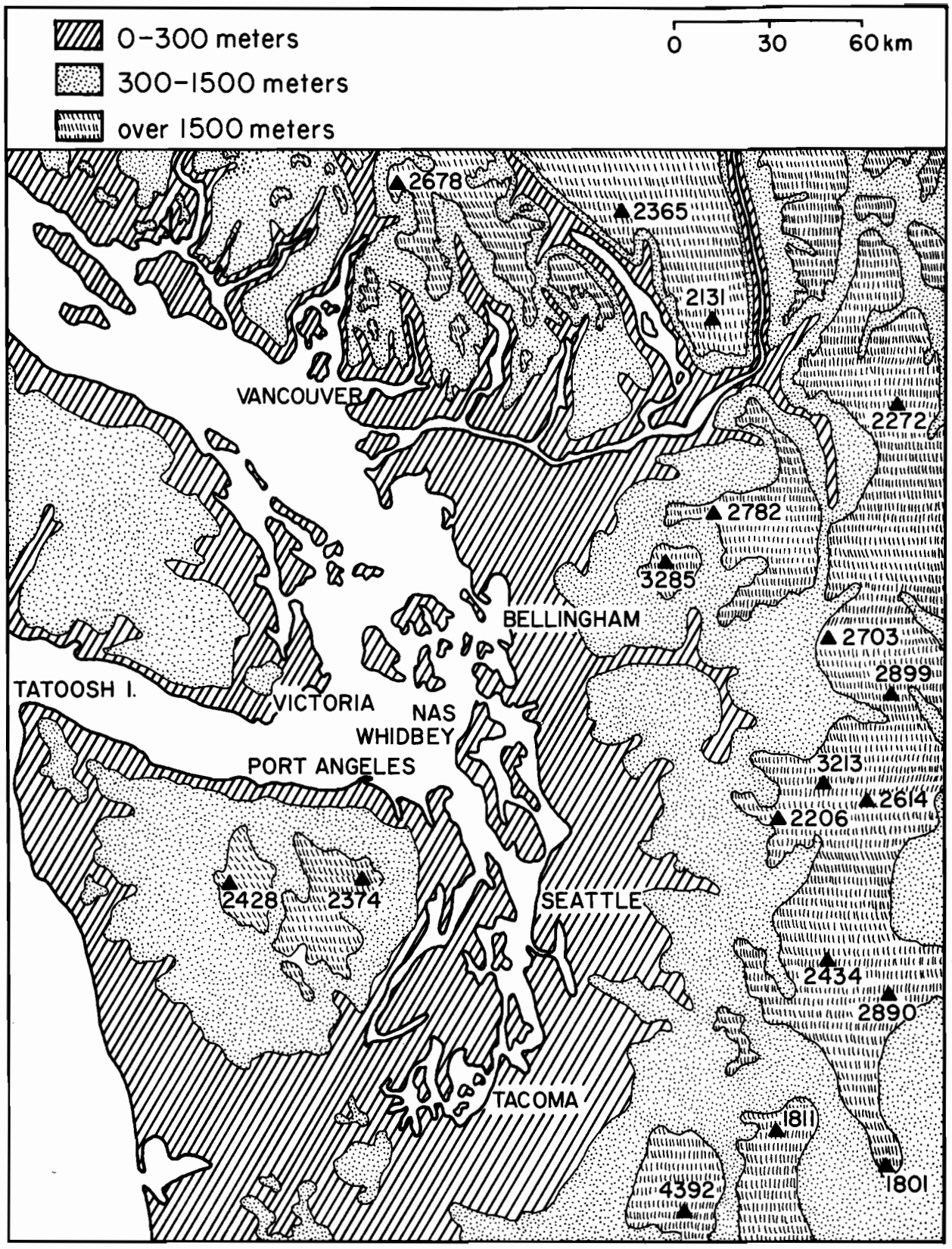

Figure 2. Topographic map of northwest Washington.

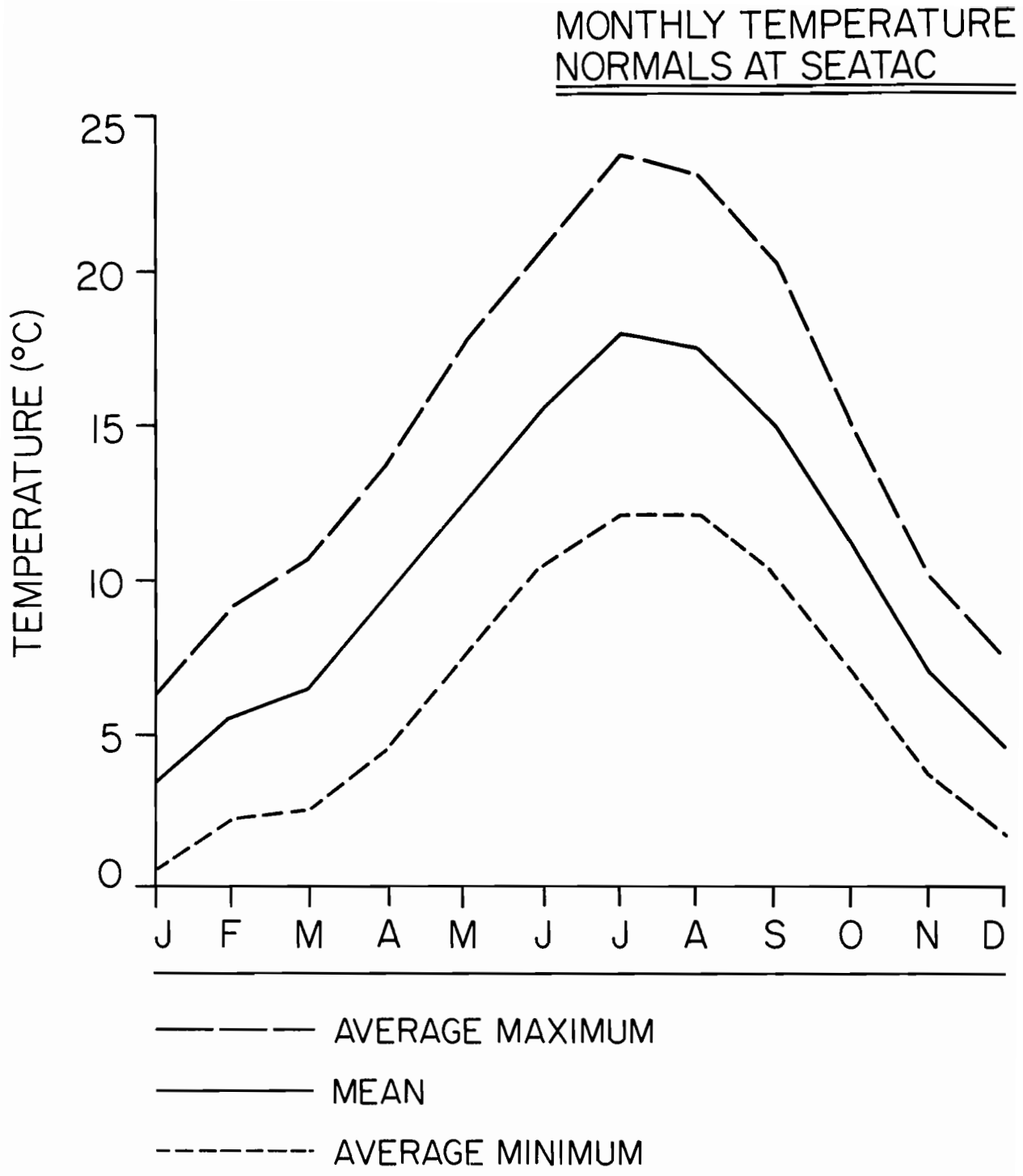

Figure 3. Annual temperature cycle at SEATAC (National Climatic Center, 1980). Values are the official normals (1945-1970).

summer months, afternoon temperatures at lower elevations are often 20°C to 25°C. Maximum temperatures reach 29°C to 32°C on a few days during a given year; temperatures of 38°C or higher occur infrequently. In winter, temperatures in the Puget Sound lowlands usually range from 3°C to 7°C in the afternoon and from -2°C to 5°C at night. Almost every winter the temperature drops to between -7°C and -12°C on a few nights, with the coldest weather occurring during a few short outbreaks of cold, dry air from the north or the east.

The longest growing season, 190 to 220 days, occurs on the San Juan Islands and in areas nearest to Puget Sound. Variations of several weeks in the duration of the growing season can occur within short distances. Near the water, the average date of the last 0°C temperature in the spring is mid-April, and the average date of the first 0°C temperature in the fall is near the end of October (Table 1). Temperatures of -2.2°C or lower are usually recorded 15 to 30 days later (Phillips, 1968).

2.2. Precipitation

The moist maritime air that reaches the Washington coast in late fall and winter is approximately the same temperature as the surface waters. Thus, orographic lifting and cooling of these air masses moving inland readily result in widespread cloudiness and precipitation. The mean annual precipitation chart for western Washington illustrates the extreme horizontal variation in precipitation (Fig. 4). The driest sections of the Sound are to the northeast of the Olympic Mountains and receive 45 to 75 cm of precipitation annually. Over most of the lowlands, annual precipitation ranges from 100 to 130 cm, increasing to 190 cm in the foothills and from 380 to 510 cm on the wettest slopes of the mountains. Due to the mild weather of the Puget Sound Basin, most of the precipitation below 500 m is in the form of rain. The yearly cycle of rainfall measured at SEATAC Airport indicates that a large variability of rainfall can be expected in any given month (Fig. 5). Fifty percent of the annual precipitation for most of the inland region falls in the four-month period from November through February. The combined rainfall for the months of July and August is less than five percent of the annual total.

Since 1900 there has been a decrease and then an increase in the long-term trend of precipitation. The ten-year mean rainfall for 1901-1910 at Seattle was 87 cm; the mean then decreased to 70 cm for 1921-1930, and has increased to 93 cm for the period 1961-1970 (Church, 1974).

Total snowfall in the Puget Sound lowlands is generally less than 25 cm per year and normally occurs from November to March, with maximum amounts in January.

2.3. Cloud cover and fog

The Puget Sound climate is characterized by a high percentage of overcast days (Fig. 6). The number of clear or partly cloudy days each month ranges from 5 to 7 in the winter, 8 to 14 in the spring and fall, and 17 or more in the summer. Table 2 gives the average total hours of sunshine and mean daily total solar radiation (in calories cm^{-2}), by month for SEATAC.

Table 1.--Probability of freezing temperatures for three stations in the Puget Sound region* (at 0°, -2.2°, -4.4°C)

		Spring Months			Fall Months		
Station	Temp.	90%	50%	10%	10%	50%	90%
Bothell	0°C	Apr 18	May 13	June 7	Sept 12	Oct 5	Oct 28
(1931-1952)	-2.2	Mar 19	Apr 13	May 8	Oct 7	Oct 30	Nov 22
	-4.4	Feb 7	Mar 8	Apr 2	Oct 22	Nov 15	-
SEATAC	0°C	Mar 15	Apr 9	May 4	Oct 10	Nov 2	Nov 25
(1945-1960)	-2.2	Feb 5	Mar 9	Apr 4	Oct 26	Nov 17	Dec 16
	-4.4	-	Feb 9	Mar 9	Nov 20	-	-
University	0°C	Feb 26	Mar 23	Apr 17	Oct 26	Nov 18	Dec 11
of	-2.2	-	Feb 2	Mar 2	Nov 21	Dec 18	-
Washington	-4.4	-	Jan 17	Feb 19	Dec 3	-	-
(1931-1960)							

*After Phillips, 1968.

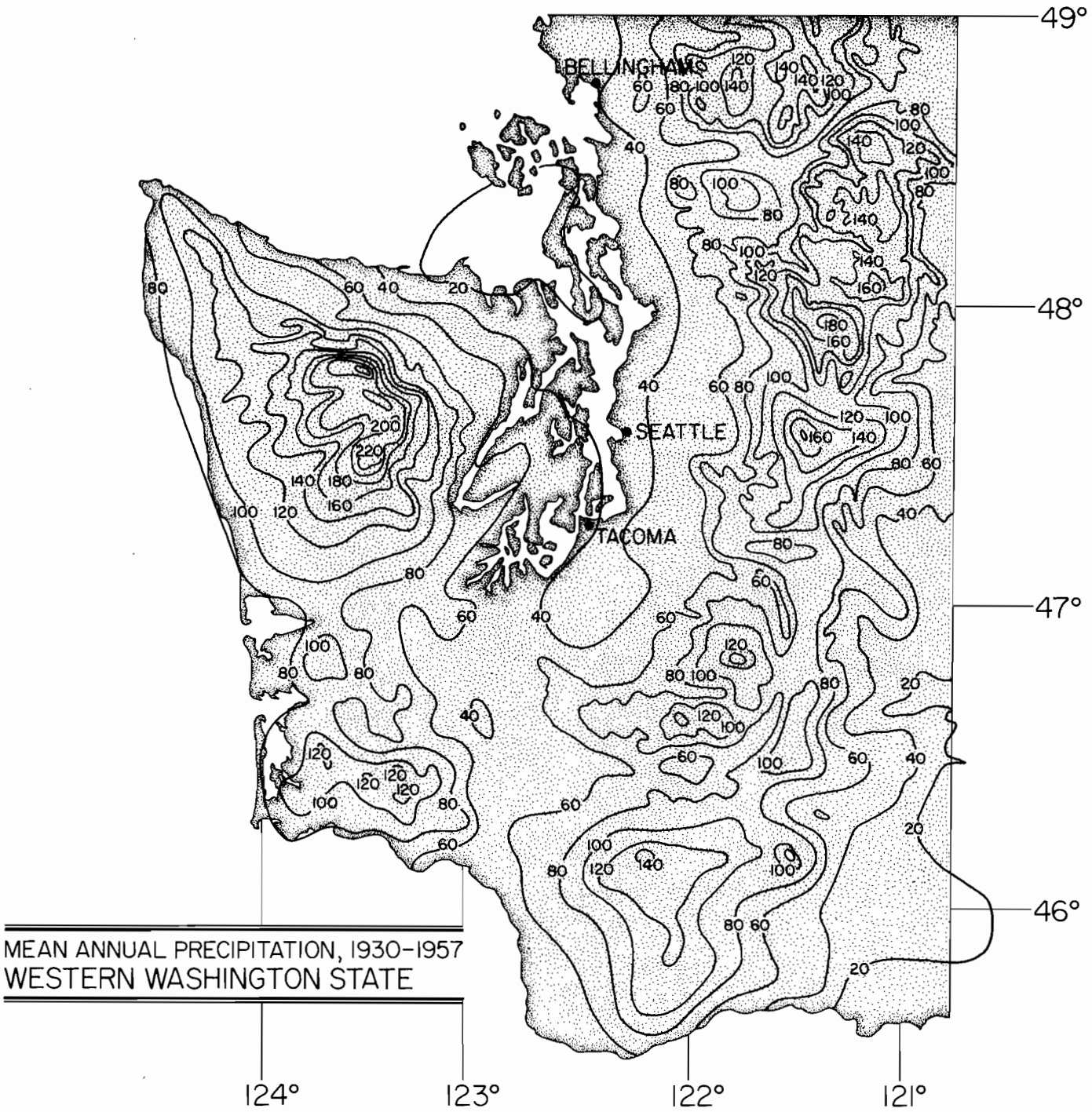

Figure 4. Mean annual precipitation (1930-1957) for western Washington. Contours are in inches (1 in = 2.54 cm). (From Philipps, 1968.)

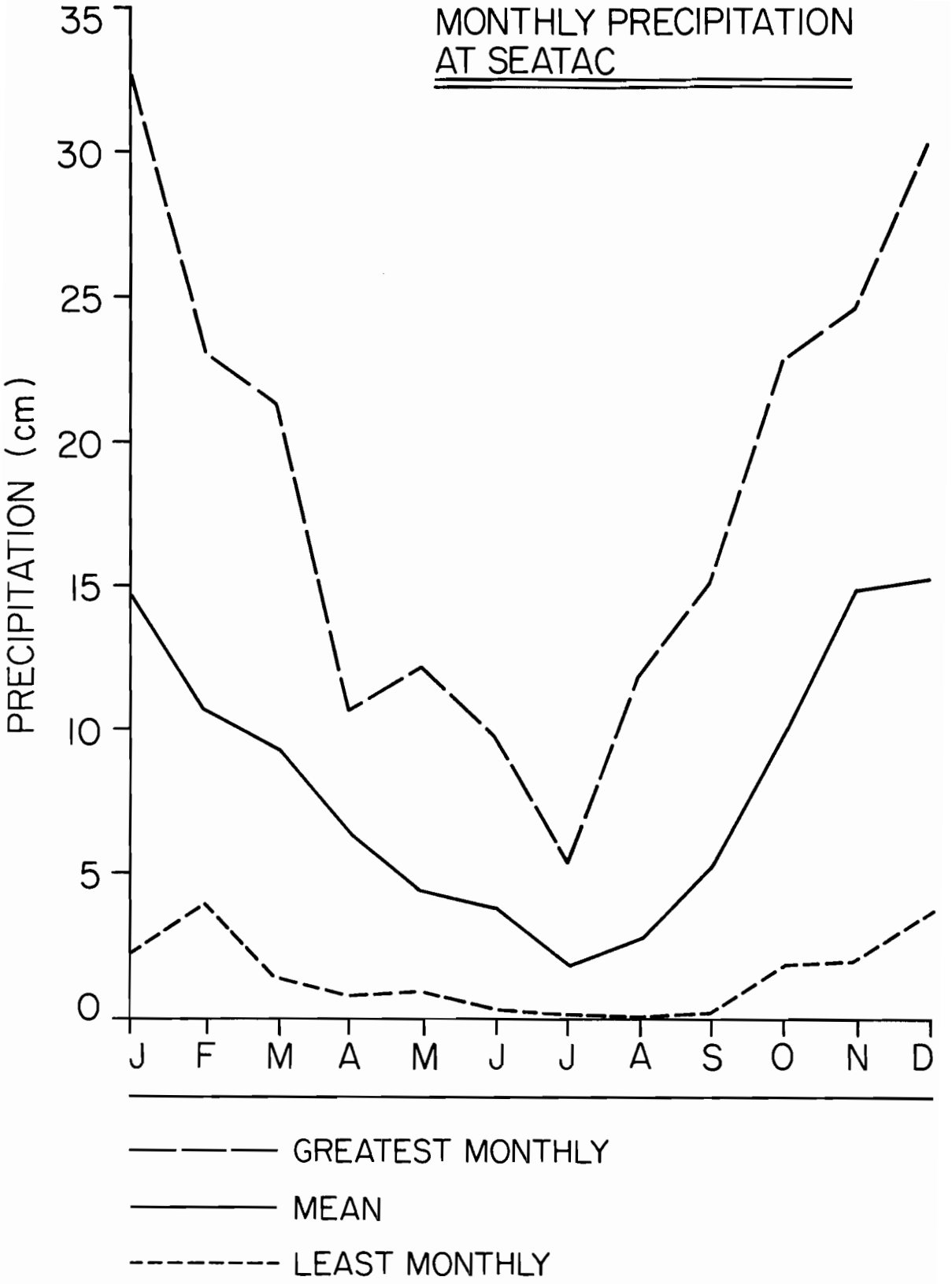

Figure 5. Annual cycle of precipitation at SEATAC (National Climatic Center, 1980). The mean is the official normal (1945-1970) and the extremes are for the period of record (1945-1980).

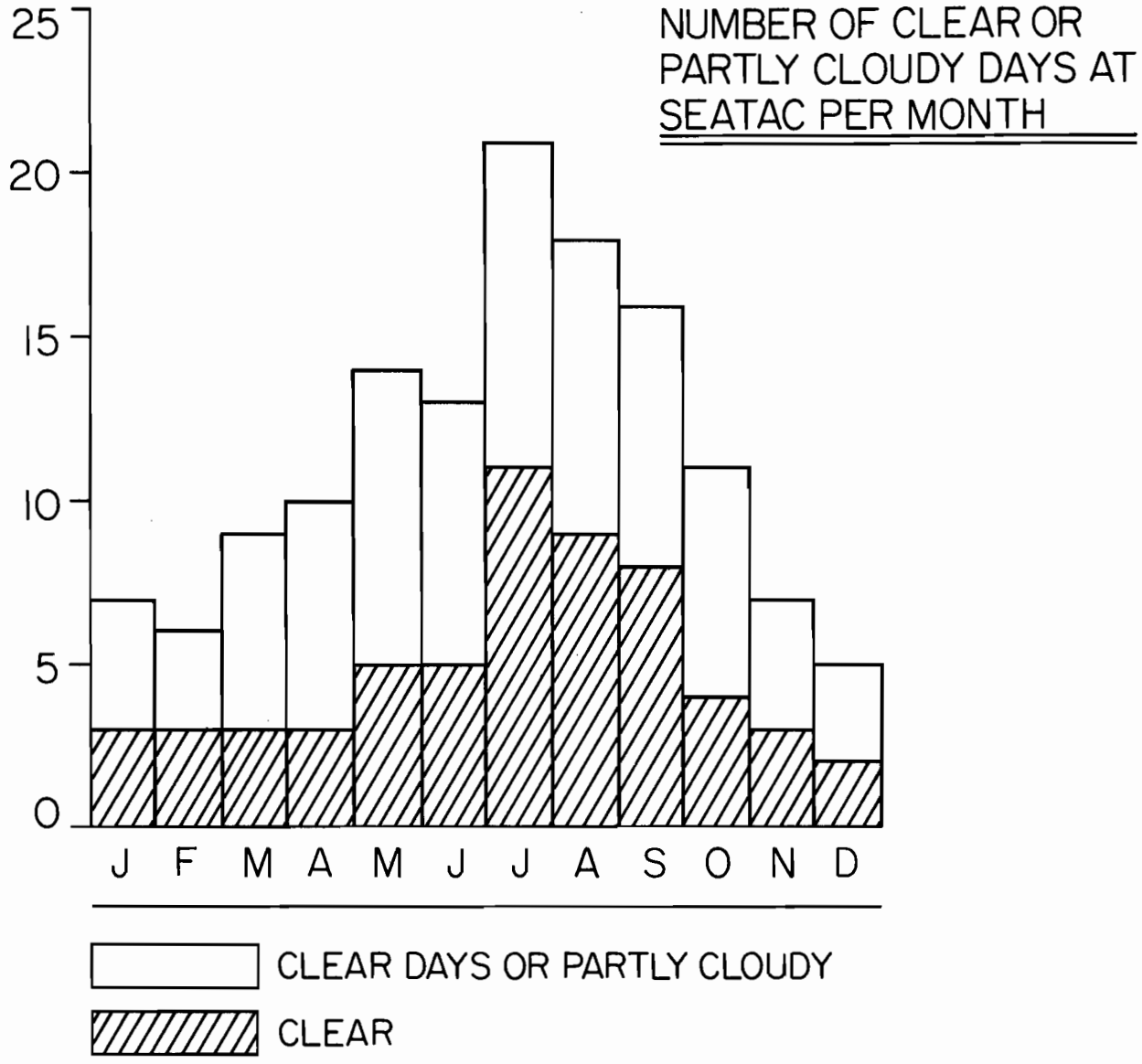

Figure 6. Annual cycle of clear or partly cloudy days (1945-1980) at SEATAC (National Climatic Center, 1980).

Table 2.--Average total hours of sunshine and mean daily total solar radiation for SEATAC Airport 1966-1975* (in Langleys, by month)

	J	F	M	A	M	J	J	A	S	O	N	D
Hours of sunshine	61	122	180	208	274	257	318	287	230	140	75	45
Total solar radiation	80	162	266	390	513	531	581	478	353	203	98	62

*After Critchfield, 1978.

Frequently during the summer and fall, fog or low clouds, 300 to 600 m thick, form over Puget Sound and the lowlands during the night and dissipate by afternoon (Table 3). In the fall, there is a high incidence of fog because of radiational cooling at night. In the summer, cool, moist coastal air is advected into the Strait of Juan de Fuca and northern Puget Sound resulting in fog formation.

2.4. Wind and waves

Puget Sound wind patterns are influenced by mountain barriers and low-level passages (Fig. 7). In southern Puget Sound the strongest winds come from the south to southwest when the more intense Pacific storms move inland. During winter, the occasional presence of high pressure over the interior of British Columbia can produce strong easterly winds blowing down pressure gradient through the Strait of Juan de Fuca (Reed, 1931). In summer, winds are generally light in the afternoons; a northerly sea breeze develops over Puget Sound and the lowlands, and a westerly sea breeze develops in the Strait of Juan de Fuca. Over the Main Basin of Puget Sound, extremes in wind speed can be expected to exceed 25 m s^{-1} once in 2 years, 40 m s^{-1} once in 50 years, and 45 m s^{-1} once in 100 years (Phillips, 1968). The wind statistics for SEATAC are given in Table 4; wind statistics for other stations, including Bellingham, Everett, and Olympia, are given in the Climatological Handbook, Columbia River Basin States (1968). A study of regional wind patterns for western Washington and southern British Columbia is given by Schoenberg (1983).

The time series of the N-S wind component and energy spectra derived from a one-year record (1975-1976) of winds at West Point, a representative location for the Puget Sound Main Basin, are shown in Fig. 8a (Cannon and Laird, 1978). The energy spectrum of both the N-S and E-W wind components for winter (Fig. 8b) shows peaks at 0.25 cycles day^{-1} (i.e., frequency of storm passage), and the spectrum for summer (Fig. 8c) has a diurnal peak in the E-W component indicating the dominant sea breeze/valley breeze influence between the Sound and the adjacent lowlands to the east.

The height and dominant period of wind-waves are a function of windspeed, wind duration, and fetch. An annual wave climatology for West Point (fig. 9) was calculated from windspeed and duration from SEATAC and fetches for Puget Sound (Skjelbreia, 1981) using relations from the Shore Protection Manual (1973). The largest waves come from the south along the major axis of the Sound during storm events. In addition, a large frequency of intermediate height waves come from the southwest; in this case wave heights are fetch-limited during the strong post-frontal southwesterly winds.

2.5. Air quality

In general, air quality problems are less serious in the Puget Sound region than in other major metropolitan regions because of the proximity of the ocean and the tendency for considerable advection north and south through Puget Sound. However, pollutants accumulate during periods of stagnation when light winds or stable stratification prevail. Since 1965, the Puget Sound Air Pollution Control Agency has operated a network of monitoring stations throughout the Puget Sound region to measure suspended particulates and concentrations of SO_2, CO, and O_3.

Table 3.--Percentage frequency of occurrence of fog for all observations by month*

	J	F	M	A	M	J	J	A	S	O	N	D	Ann
Bellingham	8.4	5.9	3.2	1.3	1.7	2.1	2.4	4.5	10.0	17.4	10.7	5.1	6.0
Hoquiam	20.2	19.7	12.6	10.0	4.9	7.5	8.5	11.9	14.9	19.5	28.6	26.8	15.2
Pt. Angeles	1.9	5.1	1.7	0.9	2.8	6.7	11.8	15.2	16.3	15.6	6.1	5.1	7.5
Everett	21.8	20.7	12.1	7.7	7.0	12.5	11.7	15.6	20.8	29.6	28.2	23.8	17.6
Olympia	23.5	23.2	14.7	8.4	4.1	4.8	6.0	9.9	17.9	28.8	30.4	25.8	16.4
Sea Boeing	13.7	11.3	6.1	3.7	1.9	2.7	3.2	4.9	12.1	17.5	20.7	14.5	9.3
SEATAC	13.7	12.5	6.7	4.4	3.1	4.6	6.9	7.8	14.8	20.3	21.2	14.5	10.9
Whidbey	5.6	8.7	4.0	2.6	2.5	4.5	8.4	10.3	14.1	20.7	15.9	6.6	8.7
Tatoosh	7.9	9.2	5.7	6.1	8.1	14.6	22.8	23.7	19.7	10.6	7.6	9.9	12.2

* From the Climatological Handbook, 1968. Most stations represent records for 1949-1958.

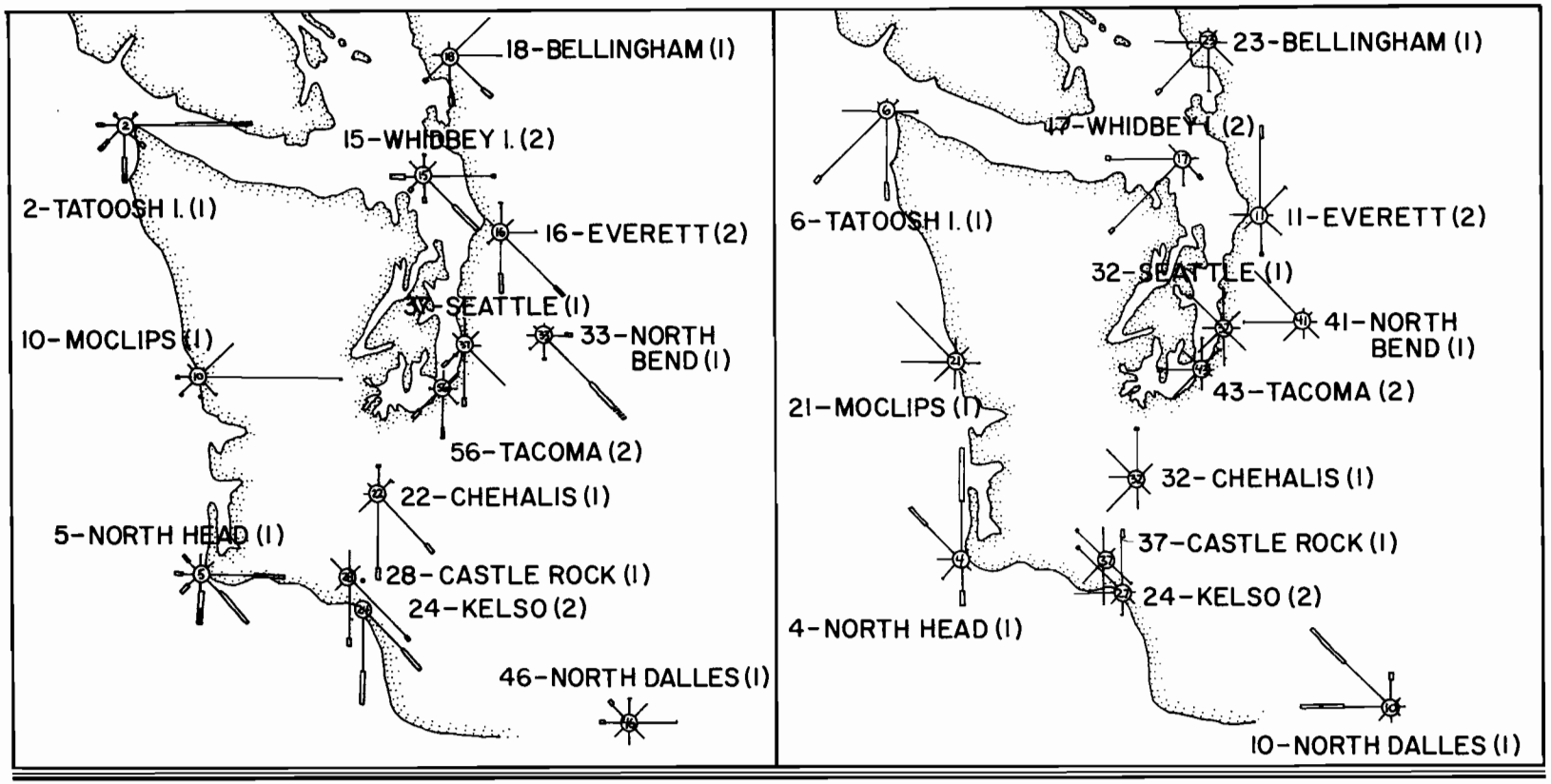

Figure 7. January and July surface wind roses for western Washington (after Phillips, 1968). This figure must be interpreted with some care as strongest winds at each station do not necessarily occur during the same synoptic event.

Table 4.--Monthly wind speed/direction frequencies* (1949-1958) for SEATAC

JANUARY

HOURLY OBSERVATIONS OF WIND SPEED MILES PER HOUR

DIR	1 TO 3	4 TO 7	8 TO 12	13 TO 18	19 TO 24	25 TO 31	32 TO 38	39 TO 46	OVER 46	TOTAL	AVE SPEED
N	3.6	3.9	2.5	1.5	0.5	0.1				6.0	11.0
NNE	3.3	1.9	2.8	2.1	0.3	*				6.5	11.2
NE	3.7	1.7	2.2	0.7	*					5.4	8.2
ENE	0.4	0.7	0.6	0.1						1.7	7.0
E	1.1	2.0	2.2	0.8	0.1					6.1	8.0
ESE	1.0	3.0	4.9	1.2	0.1	*				10.1	8.6
SE	1.3	3.7	4.6	1.0	*					10.7	7.9
SSE	0.4	1.8	2.6	0.6	0.1					5.6	8.7
S	0.3	1.5	3.7	3.0	0.9	0.2				9.6	12.2
SSW	0.2	0.8	3.7	5.4	2.2	0.4	0.1	*		12.8	14.7
SW	0.3	0.7	2.3	4.1	2.6	0.7	*			10.8	15.6
WSW	0.2	0.4	0.7	0.6	0.3	0.2	*			2.3	13.2
W	0.1	0.3	0.2	*	*	*				0.7	7.5
WNW	0.2	0.1	0.1	*						0.4	5.8
NW	0.1	0.2	0.1	*	*					0.5	7.1
NNW	0.3	0.4	0.4	0.3	0.1	*				1.5	9.6
CALM	9.3									9.3	
TOTAL	16.6	19.2	33.5	21.6	7.3	1.6	0.1	*		100.0	9.9

FEBRUARY

HOURLY OBSERVATIONS OF WIND SPEED MILES PER HOUR

DIR	1 TO 3	4 TO 7	8 TO 12	13 TO 18	19 TO 24	25 TO 31	32 TO 38	39 TO 46	OVER 46	TOTAL	AVE SPEED
N	0.4	0.9	2.0	1.5	0.3	0.1				5.2	11.2
NNE	0.4	1.1	2.9	1.7	0.2					6.3	10.6
NE	0.5	1.4	1.9	0.6	*					4.5	8.5
ENE	0.3	0.7	0.7	0.1						1.8	7.0
E	0.7	1.4	1.7	0.6						4.3	7.8
ESE	0.6	2.8	2.9	1.0	0.1					7.5	8.5
SE	0.6	2.7	3.3	0.5	*					7.2	7.9
SSE	0.3	2.0	2.2	0.6	0.1	*				5.4	8.7
S	0.4	1.7	3.5	2.9	0.7	0.2				9.3	11.6
SSW	0.4	1.1	3.7	6.1	2.8	0.6	0.1	*		14.9	14.8
SW	0.3	0.9	2.8	4.6	3.3	0.7				12.7	15.5
WSW	0.3	0.7	0.8	1.0	0.6	0.3			*	3.5	13.3
W	0.2	0.4	0.5	0.1	0.1	*				1.3	8.5
WNW	0.2	0.5	0.2	*	*					0.9	6.0
NW	0.2	0.6	0.3	*	*					1.2	6.7
NNW	0.1	0.7	1.0	0.4	0.1	*	*			2.4	10.1
CALM	11.6									11.6	
TOTAL	17.4	19.6	30.6	22.0	8.4	1.9	0.1	*	*	100.0	10.0

MARCH

HOURLY OBSERVATIONS OF WIND SPEED MILES PER HOUR

DIR	1 TO 3	4 TO 7	8 TO 12	13 TO 18	19 TO 24	25 TO 31	32 TO 38	39 TO 46	OVER 46	TOTAL	AVE SPEED
N	0.2	0.8	2.2	1.7	0.2					5.1	11.1
NNE	0.4	1.0	2.7	1.5	0.2					5.8	10.2
NE	0.6	1.2	2.0	0.7	*					4.5	8.5
ENE	0.3	0.8	0.9	0.2	*					2.2	7.9
E	0.8	1.5	1.4	0.8	0.1					4.6	8.5
ESE	0.9	2.3	3.2	1.0	0.1					7.5	8.5
SE	0.8	2.9	2.6	0.5	*					6.8	7.6
SSE	0.5	1.7	2.0	0.6	0.1					4.8	8.6
S	0.5	1.8	3.2	2.1	0.4	0.1				8.1	10.7
SSW	0.3	1.4	4.5	5.4	1.8	0.2	*			13.7	13.4
SW	0.3	1.1	4.0	5.6	3.8	0.9	*			15.7	15.3
WSW	0.1	0.9	1.5	1.7	0.9	0.2	*			5.5	13.5
W	0.1	0.6	0.8	0.3	0.1	*				1.9	9.8
WNW	0.3	0.8	0.6	*						1.7	6.5
NW	0.3	0.6	0.7	0.1						1.6	7.3
NNW	0.2	0.6	0.9	0.7	0.1					2.5	10.1
CALM	8.0									8.0	
TOTAL	14.5	19.8	33.1	23.1	7.9	1.5	0.1			100.0	10.2

APRIL

HOURLY OBSERVATIONS OF WIND SPEED MILES PER HOUR

DIR	1 TO 3	4 TO 7	8 TO 12	13 TO 18	19 TO 24	25 TO 31	32 TO 38	39 TO 46	OVER 46	TOTAL	AVE SPEED
N	0.4	1.1	3.1	2.1	0.3	0.1				6.9	10.9
NNE	0.2	1.2	3.3	2.0	0.3					7.0	11.0
NE	0.5	1.8	2.8	1.2	0.1					6.4	9.1
ENE	0.3	0.8	1.0	0.2	*					2.3	7.9
E	0.5	1.0	1.0	0.3	*					2.8	7.5
ESE	0.3	1.8	1.1	0.3	0.1					3.5	7.6
SE	0.7	2.3	2.2	0.4						5.5	7.4
SSE	0.3	1.6	1.9	0.5	0.1	*				4.3	8.8
S	0.4	1.6	2.6	1.8	0.3	0.1				6.9	10.6
SSW	0.3	1.4	3.9	3.7	0.9	0.1				10.3	12.2
SW	0.3	1.4	4.4	5.9	3.2	0.5	*			16.0	14.4
WSW	0.3	1.3	2.3	2.2	0.8	0.1	*			6.9	12.4
W	0.5	0.9	1.3	0.6	0.1	*				3.4	9.0
WNW	0.3	0.8	0.9	0.2						2.2	7.8
NW	0.3	0.9	1.3	0.3	*					2.9	8.6
NNW	0.3	0.8	1.2	1.4	0.1	*				3.8	10.9
CALM	8.8									8.8	
TOTAL	14.6	20.6	34.2	23.1	6.4	1.1	0.1			100.0	9.8

MAY

HOURLY OBSERVATIONS OF WIND SPEED MILES PER HOUR

DIR	1 TO 3	4 TO 7	8 TO 12	13 TO 18	19 TO 24	25 TO 31	32 TO 38	39 TO 46	OVER 46	TOTAL	AVE SPEED
N	0.4	1.3	4.6	2.7	0.1					9.1	10.6
NNE	0.3	1.5	3.8	1.9	0.1					7.6	10.3
NE	0.4	1.7	3.9	1.9	0.1					8.0	9.9
ENE	0.2	0.7	0.9	0.2						2.0	8.1
E	0.5	0.8	0.7	0.1						2.1	6.5
ESE	0.4	1.1	0.9	0.1						2.6	7.0
SE	0.4	1.8	1.2	0.1						3.7	6.9
SSE	0.2	1.7	1.2	0.1						3.3	7.3
S	0.3	1.9	3.0	0.5	*					5.7	8.5
SSW	0.4	2.4	4.4	2.3	0.2					9.8	10.0
SW	0.3	2.1	6.4	5.5	1.7	0.1				16.1	12.4
WSW	0.2	1.5	3.0	1.9	0.4	*				6.9	10.9
W	0.3	1.1	1.9	0.5	0.1	*				3.9	9.2
WNW	0.2	1.2	1.3	0.2						2.9	7.9
NW	0.2	1.3	2.0	0.4	*					4.0	8.5
NNW	0.2	1.0	2.2	1.6	0.1					5.1	10.5
CALM	7.6									7.6	
TOTAL	12.7	23.1	41.2	20.0	2.8	0.2				100.0	9.2

JUNE

HOURLY OBSERVATIONS OF WIND SPEED MILES PER HOUR

DIR	1 TO 3	4 TO 7	8 TO 12	13 TO 18	19 TO 24	25 TO 31	32 TO 38	39 TO 46	OVER 46	TOTAL	AVE SPEED
N	0.3	1.3	3.5	2.0	0.2					7.2	10.6
NNE	0.3	1.4	3.2	1.6	0.1					6.7	10.1
NE	0.2	1.3	2.9	1.2	0.1					5.6	9.7
ENE	0.2	0.5	0.7	0.1						1.6	7.7
E	0.3	0.6	0.6	0.1						1.5	7.1
ESE	0.4	0.8	0.4	0.1						1.8	6.2
SE	0.3	1.1	1.1	0.1						2.7	7.2
SSE	0.3	1.0	1.2	0.1						2.5	7.5
S	0.4	2.1	3.3	0.9	*					6.7	8.7
SSW	0.5	2.3	5.8	3.0	0.4	*				11.9	10.6
SW	0.4	2.9	8.8	6.9	1.3	0.2				20.4	11.8
WSW	0.3	1.9	3.6	1.8	0.2					7.9	10.1
W	0.3	1.6	2.3	0.6	*					4.8	8.7
WNW	0.3	1.3	1.6	0.2						3.5	7.7
NW	0.3	0.9	1.5	0.4						3.1	8.5
NNW	0.2	1.0	1.7	0.8	0.1					3.7	9.9
CALM	8.4									8.4	
TOTAL	13.4	21.9	42.1	20.0	2.4	0.2				100.0	9.1

* From the Climatological Handbook, 1968.

Table 4.--cont.

JULY

HOURLY OBSERVATIONS OF WIND SPEED MILES PER HOUR

DIR	1 TO 3	4 TO 7	8 TO 12	13 TO 18	19 TO 24	25 TO 31	32 TO 38	39 TO 46	OVER 46	TOTAL	AVE SPEED
N	0.4	1.7	4.5	2.2	0.1	*				8.9	10.1
NNE	0.3	1.9	5.0	1.9	0.1					9.1	10.0
NE	0.4	1.9	3.8	1.7	0.1					7.9	9.6
ENE	0.3	0.8	0.9	0.2	*					2.3	7.9
E	0.3	0.6	0.1		*					1.0	5.4
ESE	0.2	0.5	0.3							1.0	5.7
SE	0.3	0.8	0.8	*						2.0	6.6
SSE	0.2	0.9	1.1	*						2.2	7.2
S	0.4	1.7	2.7	0.5	*					5.3	8.2
SSW	0.5	2.2	5.1	1.3	0.2					9.3	9.2
SW	0.7	3.3	8.0	3.5	0.4	*				16.0	10.1
WSW	0.4	1.9	3.3	1.1	0.1					6.7	9.1
W	0.4	1.9	2.6	0.6	0.1					5.4	8.5
WNW	0.2	1.6	1.8	0.4						4.0	8.2
NW	0.3	1.4	2.1	0.7						4.5	8.7
NNW	0.2	1.2	2.8	1.4	*					5.6	10.2
CALM	8.8									8.8	
TOTAL	14.3	24.3	44.9	15.6	1.0	*				100.0	8.4

AUGUST

HOURLY OBSERVATIONS OF WIND SPEED MILES PER HOUR

DIR	1 TO 3	4 TO 7	8 TO 12	13 TO 18	19 TO 24	25 TO 31	32 TO 38	39 TO 46	OVER 46	TOTAL	AVE SPEED
N	0.4	1.4	4.7	1.4						7.9	9.6
NNE	0.5	1.7	4.2	1.6	*					8.1	9.5
NE	0.7	1.8	3.4	1.0	*					7.0	8.8
ENE	0.3	0.7	0.8	0.1						1.9	7.3
E	0.4	0.9	0.3							1.7	5.3
ESE	0.4	0.7	0.4	*						1.6	5.9
SE	0.5	1.5	1.0	*						3.0	6.5
SSE	0.3	1.7	1.1	*						3.1	6.7
S	0.8	2.2	2.9	0.3	*					6.3	7.5
SSW	0.7	2.6	4.7	1.5	0.1					9.5	9.0
SW	0.8	2.8	6.2	2.9	0.3	*				13.0	10.0
WSW	0.5	1.9	3.3	1.0	0.1	*				6.7	8.9
W	0.5	1.8	2.2	0.4	*					4.8	7.9
WNW	0.4	1.5	2.1	0.3	*					4.2	8.0
NW	0.5	1.5	2.3	0.6						4.9	8.4
NNW	0.4	1.0	3.0	1.0	*					5.5	9.5
CALM	11.0									11.0	
TOTAL	19.0	25.7	42.5	12.1	0.6	*				100.0	7.7

SEPTEMBER

HOURLY OBSERVATIONS OF WIND SPEED MILES PER HOUR

DIR	1 TO 3	4 TO 7	8 TO 12	13 TO 18	19 TO 24	25 TO 31	32 TO 38	39 TO 46	OVER 46	TOTAL	AVE SPEED
N	0.7	1.8	5.5	3.1	0.3					11.0	10.5
NNE	0.7	1.9	5.0	2.7	0.2	*				10.5	10.2
NE	0.7	2.3	3.9	1.4	0.1					8.4	9.0
ENE	0.3	0.6	0.6	0.1						1.6	6.8
E	0.5	1.3	0.5	*						2.3	5.8
ESE	0.5	1.2	1.0	*						2.8	6.6
SE	0.8	1.9	2.0	0.2						4.8	7.1
SSE	0.7	1.5	1.4	0.1	*					3.7	6.8
S	0.6	1.8	3.3	0.8	0.1	*				6.6	8.8
SSW	0.4	1.9	4.6	2.2	0.3	*	*			9.5	10.4
SW	0.6	2.2	4.4	2.7	0.6	0.1				10.6	10.6
WSW	0.5	1.3	1.4	0.6	0.1	*				3.7	9.0
W	0.3	1.2	1.2	0.3	*					2.9	7.7
WNW	0.4	1.2	0.8	0.1						2.5	6.6
NW	0.3	1.3	1.0	0.2						2.5	7.5
NNW	0.3	1.0	2.1	1.1	0.1	*				4.6	9.9
CALM	11.9									11.9	
TOTAL	20.1	23.9	38.5	15.5	1.8	0.2	*			100.0	8.1

OCTOBER

HOURLY OBSERVATIONS OF WIND SPEED MILES PER HOUR

DIR	1 TO 3	4 TO 7	8 TO 12	13 TO 18	19 TO 24	25 TO 31	32 TO 38	39 TO 46	OVER 46	TOTAL	AVE SPEED
N	0.5	2.0	4.4	1.3	*	*				8.3	9.3
NNE	0.4	2.4	4.5	2.3	0.3					9.8	10.2
NE	0.6	2.2	2.5	0.9	0.1					6.4	8.5
ENE	0.3	0.7	0.6	0.1	*					1.8	7.1
E	0.7	1.2	1.2	0.4	0.1					3.5	7.9
ESE	0.8	1.9	2.5	0.7	0.1					6.0	8.0
SE	0.6	2.5	3.9	0.7	*					7.7	8.3
SSE	0.4	1.7	2.4	0.7	0.1					5.2	8.7
S	0.5	2.2	3.8	2.8	0.8	0.1				10.3	11.1
SSW	0.4	1.4	4.1	3.7	1.4	0.3				11.3	12.9
SW	0.2	1.0	2.6	3.3	1.3	0.2				8.6	13.3
WSW	0.1	0.7	1.1	0.6	0.3	*				2.7	11.1
W	0.3	0.5	0.6	0.1	*					1.5	7.6
WNW	0.2	0.7	0.6	*						1.6	6.8
NW	0.3	0.7	0.7	0.1	*					1.8	7.3
NNW	0.2	0.7	1.2	0.4	0.1					2.6	9.1
CALM	10.9									10.9	
TOTAL	17.4	22.5	36.7	18.2	4.7	0.6				100.0	8.9

NOVEMBER

HOURLY OBSERVATIONS OF WIND SPEED MILES PER HOUR

DIR	1 TO 3	4 TO 7	8 TO 12	13 TO 18	19 TO 24	25 TO 31	32 TO 38	39 TO 46	OVER 46	TOTAL	AVE SPEED
N	0.5	1.2	3.0	1.8	0.3	*	*			6.8	10.6
NNE	0.4	1.4	3.0	2.0	0.1	0.1				7.0	10.3
NE	0.3	1.1	1.8	0.9	*					4.1	9.4
ENE	0.3	0.6	0.7	0.2						1.7	7.7
E	0.8	1.4	1.4	0.4						4.0	7.3
ESE	0.8	2.1	3.6	1.3	0.2					7.9	9.1
SE	0.8	3.5	5.2	1.4	0.1					11.0	8.5
SSE	0.5	2.0	2.8	1.0	0.1					6.5	8.8
S	0.5	1.9	3.6	2.9	0.8	0.2	0.1	*		9.9	11.5
SSW	0.4	1.0	2.7	3.7	1.9	0.4				10.1	14.0
SW	0.3	1.1	2.3	3.2	1.9	0.6	0.1			9.5	14.6
WSW	0.3	0.6	0.7	0.6	0.4	0.1	*			2.7	12.3
W	0.3	0.4	0.3	0.1		*				1.0	7.0
WNW	0.2	0.3	0.2	*						0.7	5.9
NW	0.2	0.4	0.4	0.1	*	0.1	*			1.2	8.8
NNW	0.3	0.5	0.7	0.1	*	*				1.7	8.1
CALM	14.0									14.0	
TOTAL	21.0	19.5	32.3	19.6	6.0	1.5	0.2	*		100.0	9.1

DECEMBER

HOURLY OBSERVATIONS OF WIND SPEED MILES PER HOUR

DIR	1 TO 3	4 TO 7	8 TO 12	13 TO 18	19 TO 24	25 TO 31	32 TO 38	39 TO 46	OVER 46	TOTAL	AVE SPEED
N	0.2	0.9	1.5	0.9	0.2					3.8	10.3
NNE	0.3	0.9	2.4	1.9	0.3					5.8	11.0
NE	0.3	1.0	1.5	0.6	*					3.4	8.9
ENE	0.2	0.6	0.3	0.1	*					1.3	7.6
E	0.8	1.4	1.5	0.8	0.2					4.7	8.5
ESE	0.7	2.0	3.5	2.1	0.3	*				8.5	10.0
SE	0.6	3.3	4.4	1.6	0.1					10.1	8.9
SSE	0.4	1.7	3.0	1.1	0.1					6.4	9.3
S	0.5	2.2	4.4	4.4	1.4	0.3				13.2	12.3
SSW	0.2	1.2	3.9	6.5	3.4	0.8	0.1			16.1	15.1
SW	0.4	1.0	3.0	3.9	3.1	1.1	0.2			12.6	15.7
WSW	0.1	0.2	0.5	0.6	0.2	0.2	*	*		1.7	13.7
W	0.2	0.3	0.2	0.1	*	*				0.8	8.6
WNW	0.1	0.1	0.1							0.4	6.4
NW	0.1	0.2	0.1	*	*					0.4	7.6
NNW	0.1	0.2	0.2	0.1	*					0.7	8.8
CALM	10.2									10.2	
TOTAL	15.4	17.4	30.6	24.7	9.3	2.4	0.3	*		100.0	10.6

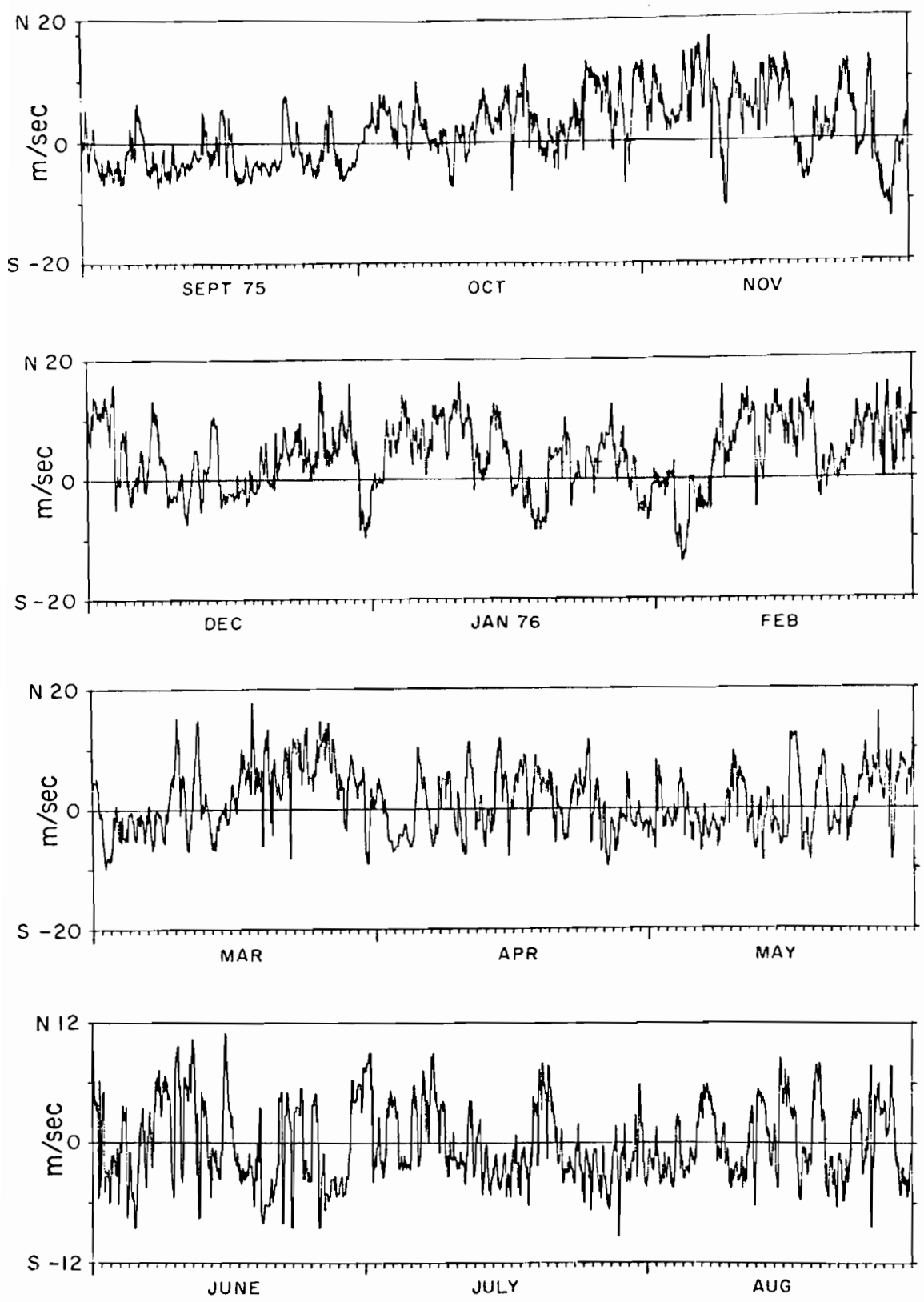

Figure 8a. One-year time series of the N-S wind component for West Point. For this chart a positive north component means the wind is from the south (Cannon and Laird, 1978).

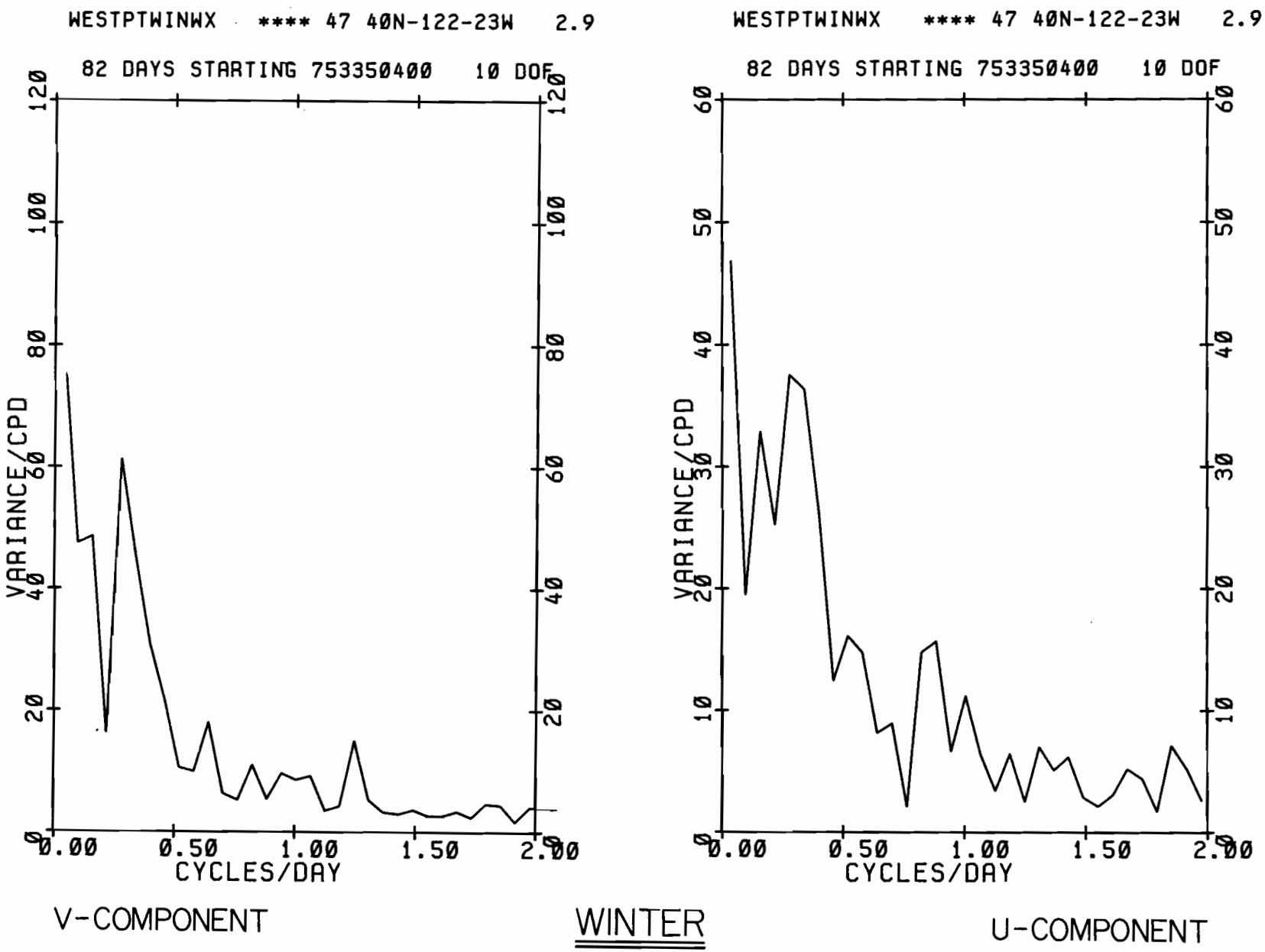

Figure 8b. Frequency spectra for the north (v) and east (u) component of wind for West Point during winter (December-February) (Cannon and Laird, 1978).

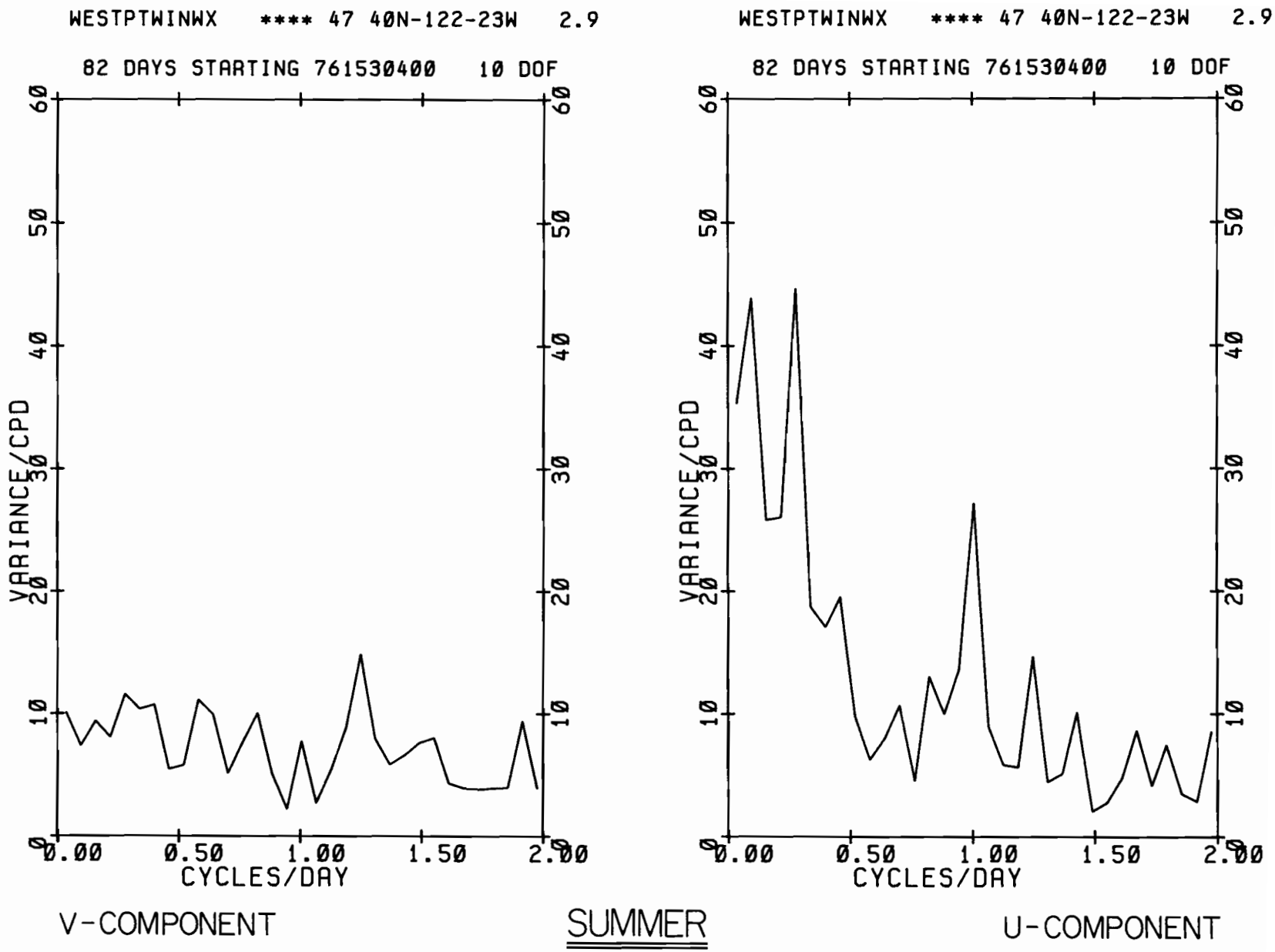

Figure 8c. Frequency spectra for the north (v) and east (u) component of wind for West Point during summer (June-August) (Cannon and Laird, 1978).

WEST POINT WIND-WAVE ROSE

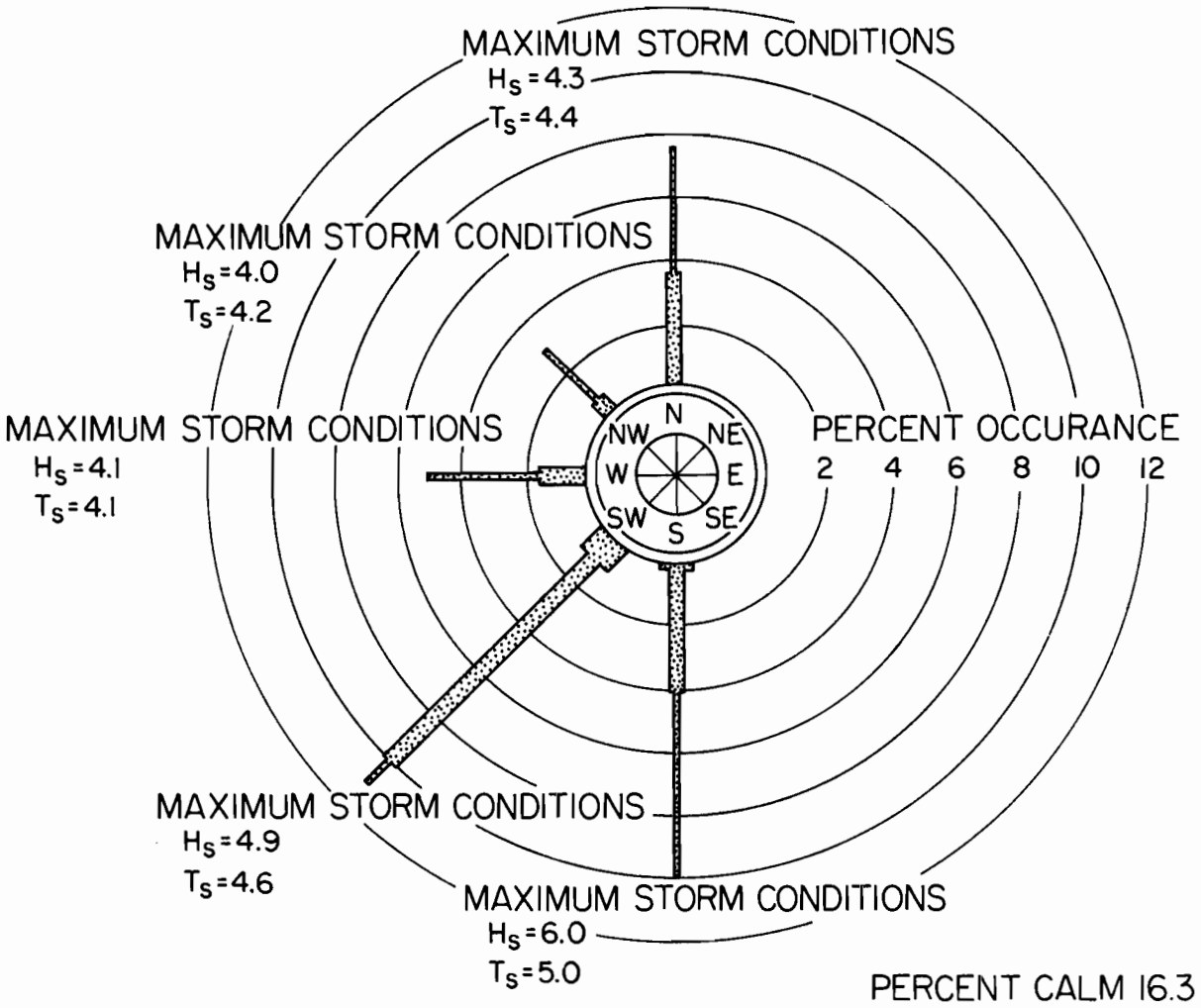

LEGEND

CHARACTERISTIC WAVE

H_S (ft)

T_S (sec)

UP TO 1.0, T_S = 2.0

H_S = 1.0, T_S = 2.0 TO H_S = 2.5, T_S = 3.5

OVER H_S = 2.5, T_S = 3.5

Figure 9. Annual wave climatology computed for West Point from the wind climatology at SEATAC (Skjelbreia, 1981).

Suspended particulate concentrations in the air over the industrialized Duwamish Valley and the tide flats of Tacoma have regularly exceeded established local and national standards since monitoring was initiated (Table 5 and Fig. 10). The long-term trend in suspended particulate concentrations over the region decreased until 1976 and then leveled off or increased slightly from 1976 to 1979. Increases in particulates were observed in both industrial and suburban residential areas in 1979, with seven stations exceeding the national standard of 75 $\mu g\ m^{-3}$. Monthly averages above 160 $\mu g\ m^{-3}$ have been measured in the two major industrialized areas.

Of the stations monitoring ozone concentrations, four of ten in 1978 and seven of nine in 1979 measured levels that exceeded national standards. Ozone concentrations are higher in summer months due to more hours of sunlight per day, with maximum concentration normally occurring 10-30 km southeast of major urban centers.

Of the stations monitoring CO concentrations, ten of twelve in 1978 and nine of thirteen in 1979 reported levels that on at least two occasions exceeded an 8-hour average of 9 ppm, the national standard. High ambient levels of CO occur near congested areas where there is slow-moving motor vehicle traffic and when low-level winds are light and stable meteorological conditions exist.

Table 5.--Annual average concentration of suspended particulates[1] for stations in the Puget Sound region 1972-1979*

Year	Everett	Duwamish	Tacoma	Auburn
1972	60	97	94	55
1973	53	111	82	63
1974	40	77	69	51
1975	36	66	54	38
1976	45	83	87	49
1977	43	94	91	54
1978	45	100	98	54
1979	50	101	107	62

[1]($\mu g\ m^{-3}$).
*(Puget Sound Air Pollution Control Agency, 1972-1980).

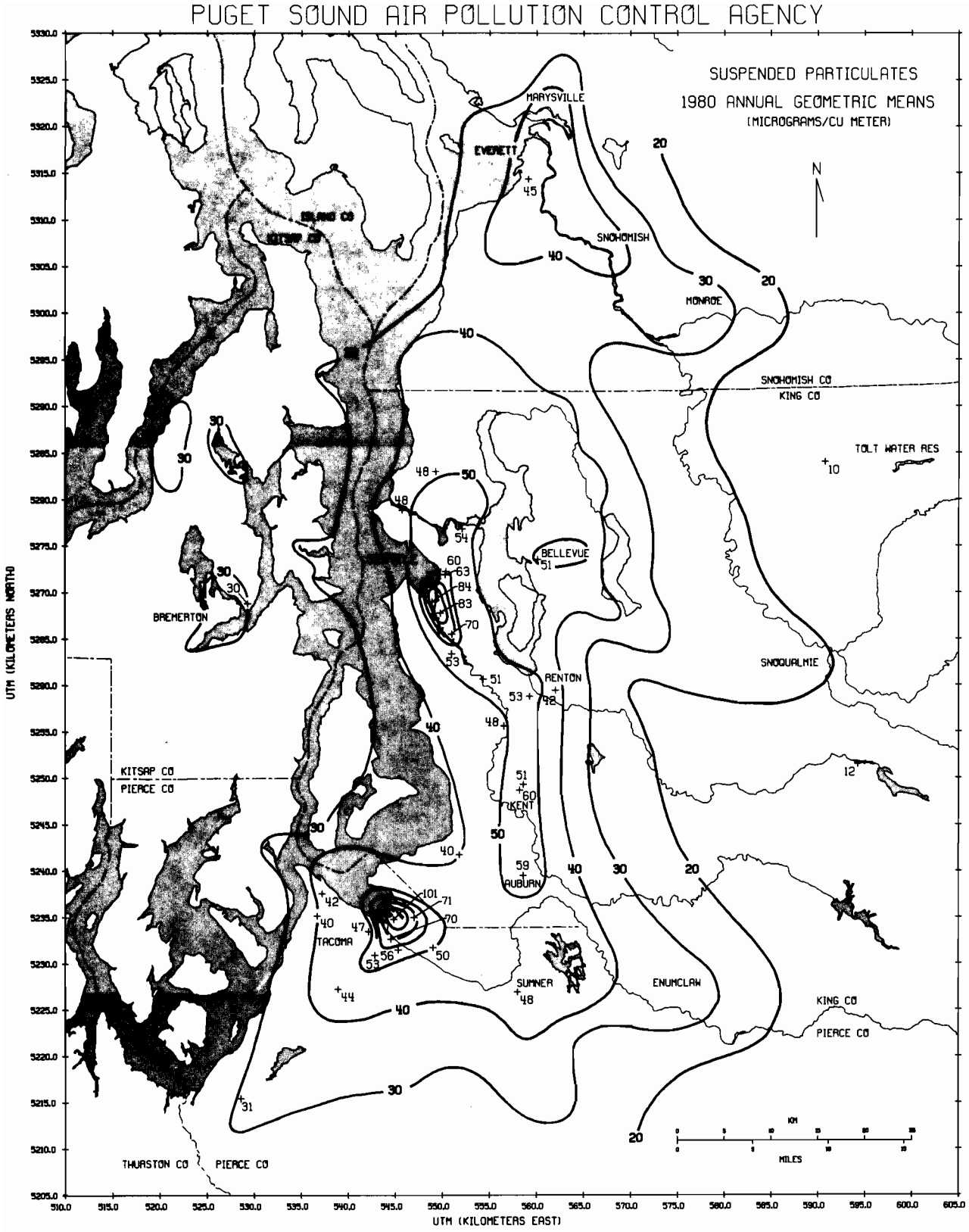

Figure 10. Mean annual particulate concentration for 1980 (Puget Sound Air Pollution Control Agency, 1980).

2.6. Surface hydrology

The mean annual flow for the major rivers of the Puget Sound region varies greatly with locality (Williams et al., 1982). By far the largest input is from the northern tributaries, with the Skagit River being the largest single source (Fig. 11).

There are two periods of high stream flow each year (Fig. 12). One occurs during the fall and winter, coinciding with the season of maximum precipitation. The other, in late spring and early summer, is caused by snow melt in the mountains, augmented by rainfall. Streams rise to near or above flood stage several times during each rainy season; the highest flood crests occur in late fall and early winter. Stream flow also shows large variability from year to year (Fig. 12b).

3. Large-scale Meteorological Characteristics

Throughout the winter the synoptic (large-scale) meteorology over Puget Sound is characterized by a sequence of cyclonic (low sea-level pressure) disturbances (Klein, 1957) that move over or to the north of the region. This sequence is interrupted infrequently by anticyclones (high sea-level pressure regions). Spring and autumn are transition periods when the frequency and intensity of cyclones diminish and increase respectively. Summer is marked by light cyclonic activity and by long periods of anticyclonic influence due to the intrusion of a high-pressure region from the north Pacific.

Winter cyclone tracks for the Northeast Pacific indicate that most of the air masses affecting Puget Sound have their origin in the central Pacific. While it is difficult to generalize all synoptic weather charts, two typical storm types suggest themselves (Reed, 1932). In the first type, designated L1 (Fig. 13a), pressure patterns are associated with a large and extensive low-pressure area in the Gulf of Alaska and a series of accompanying cold frontal systems. The center of the low pressure usually drifts slowly, whereas the frontal systems advect rapidly across the Pacific, rotating about the center of the low. The warm sector ahead of the front is usually of small extent by the time it is in the vicinity of the coast; therefore, classical warm fronts are often weak and diffuse although they are still associated with stable air masses.

As the storms approach the coast, they are modified by the effect of the continent (Lau, 1979). The surface features of the cold front in L1 often rapidly approach the coast and slow, while higher level features continue to move over Puget Sound. The severity of the weather associated with the front is not always as great as it is when the storm system is over the Pacific. Thus, it is often difficult to forecast the timing and severity of frontal features over Puget Sound by extrapolating the speed of the storm while it is over the Pacific. The CYCLES project is an extensive study of the mesoscale and microscale organization and structure of clouds and precipitation in storms affecting western Washington (Hobbs, 1978; Hobbs et al., 1980; Parsons and Hobbs, 1982).

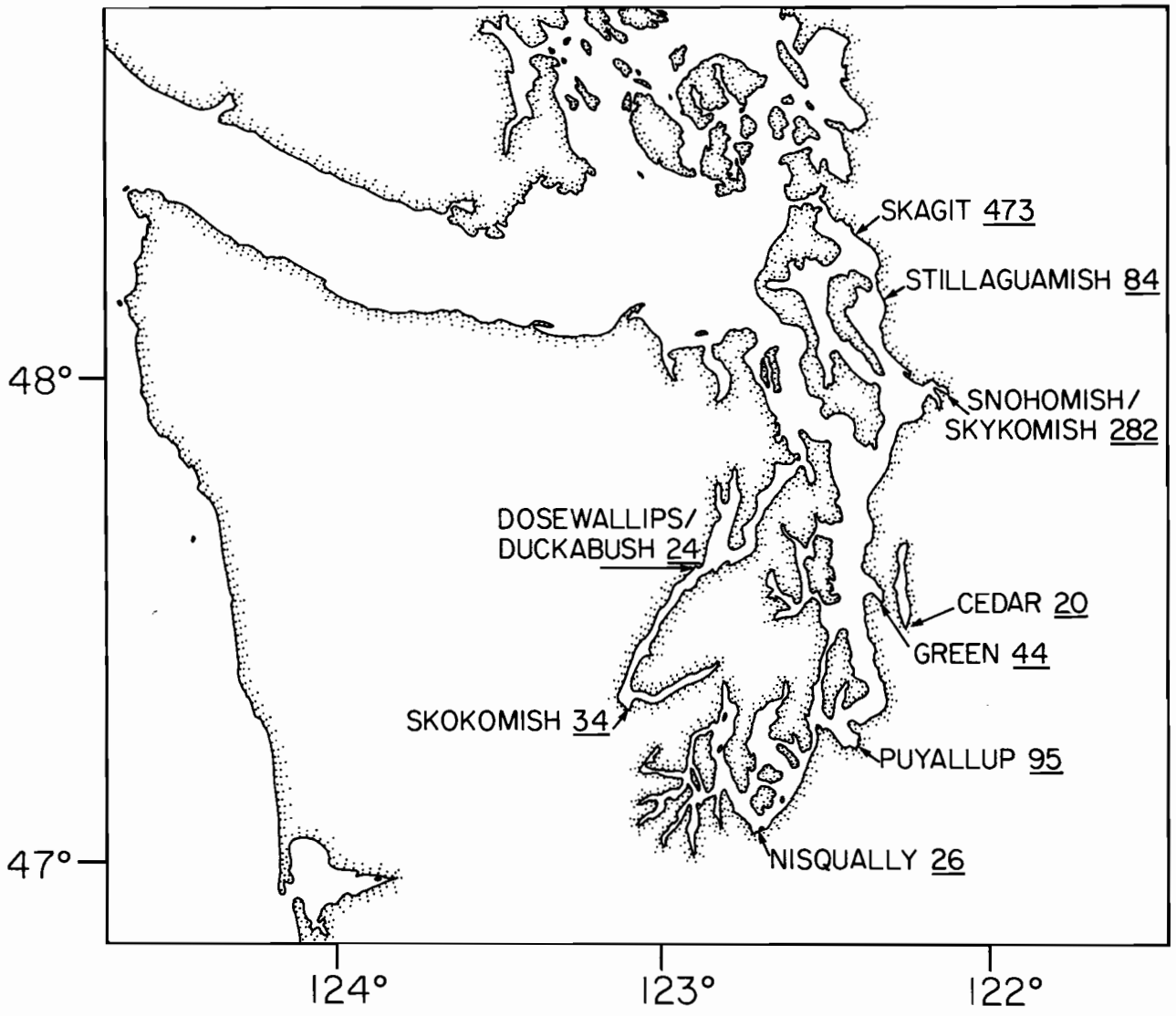

Figure 11. Mean annual runoff (m^3 s^{-1}) for Puget Sound. Periods of record vary (Williams et al., 1982).

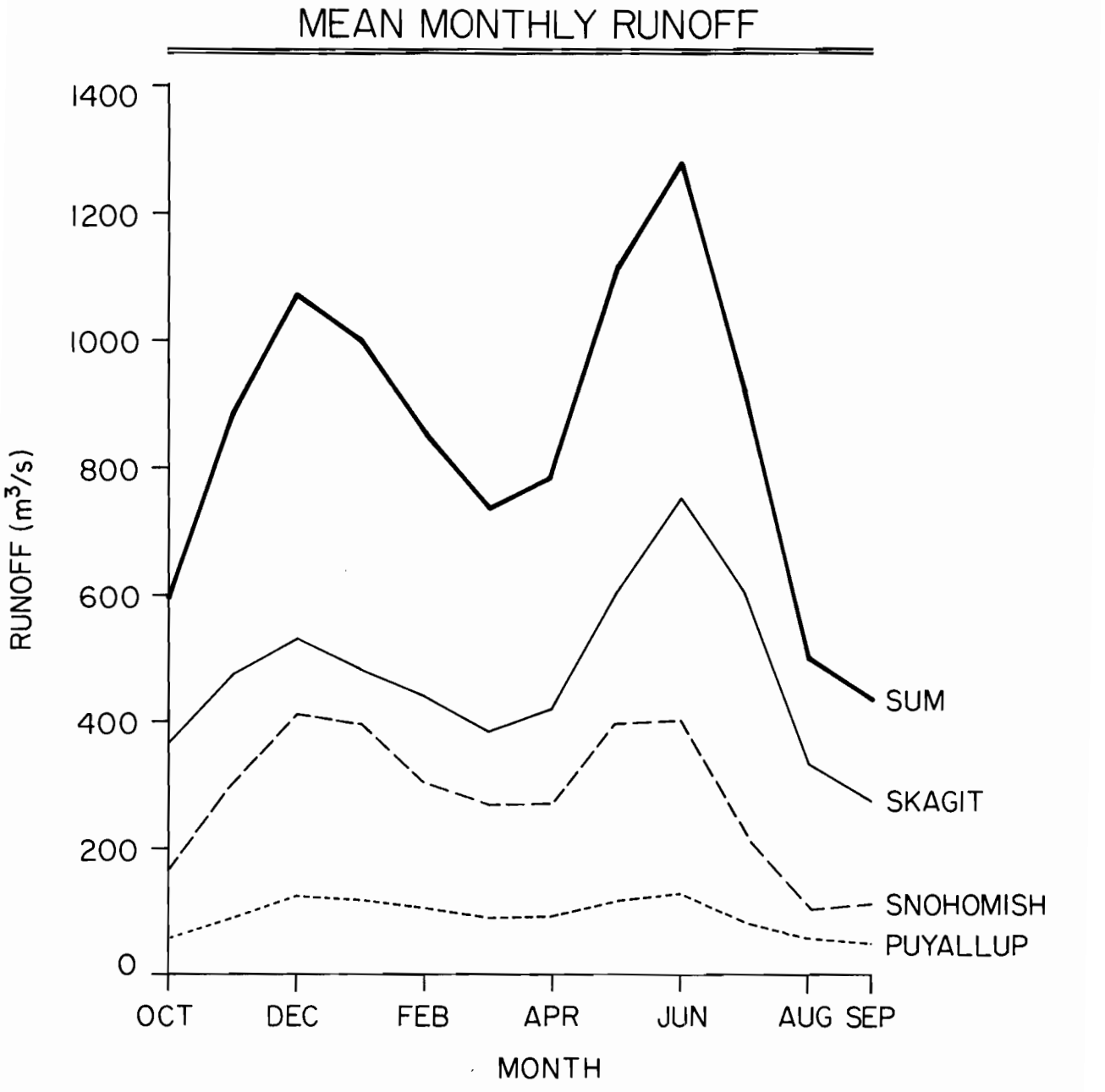

Figure 12a. Mean annual cycle of discharge for Puget Sound's three major tributaries (Williams et al., 1982). The period of record for the Skagit was 1941-1979, the period for the Snohomish was 1963-1979, and the period for the Puyallup was 1914-1979.

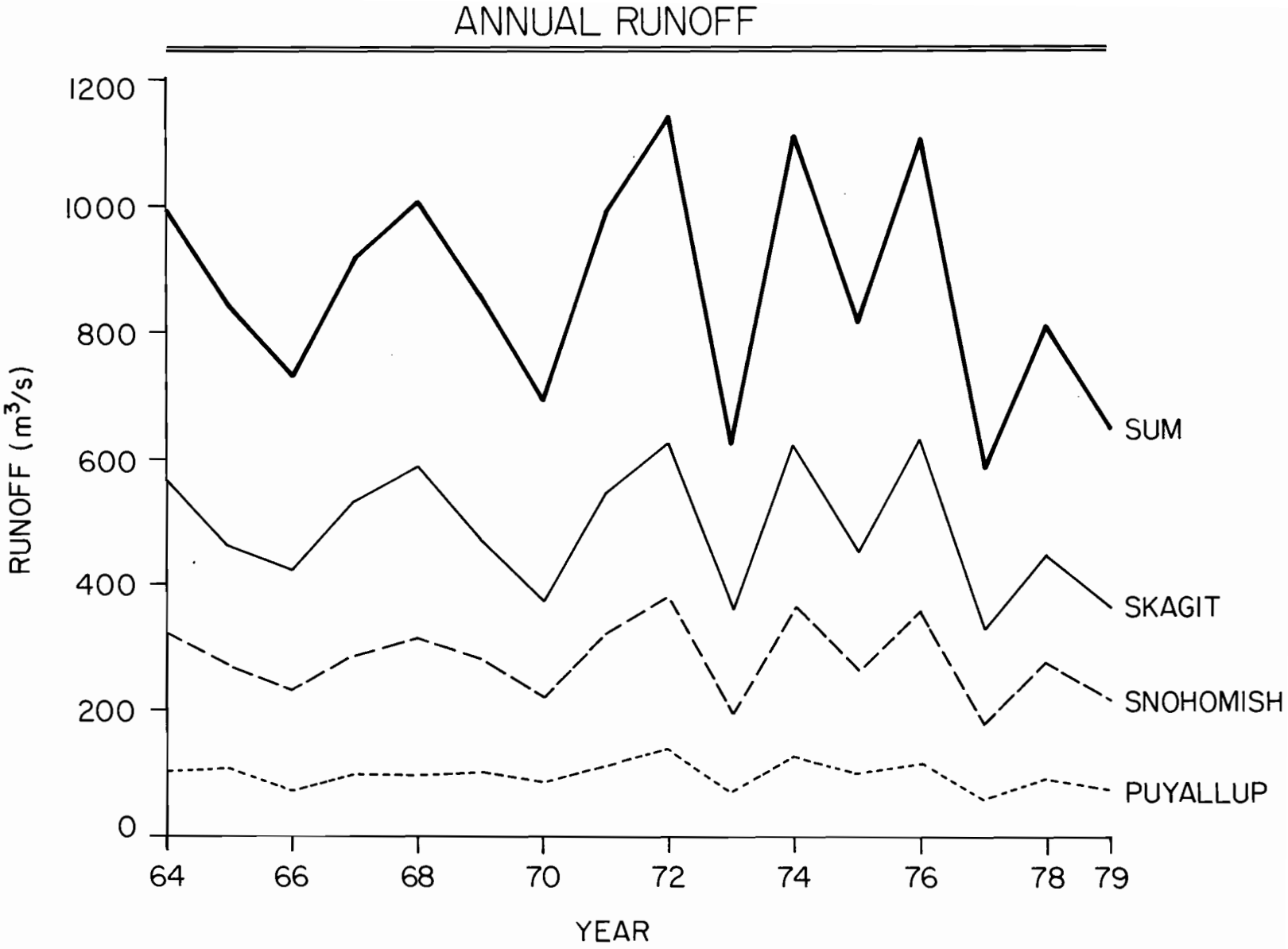

Figure 12b. Interannual variability of discharge for Puget Sound's three major tributaries (Williams et al., 1982).

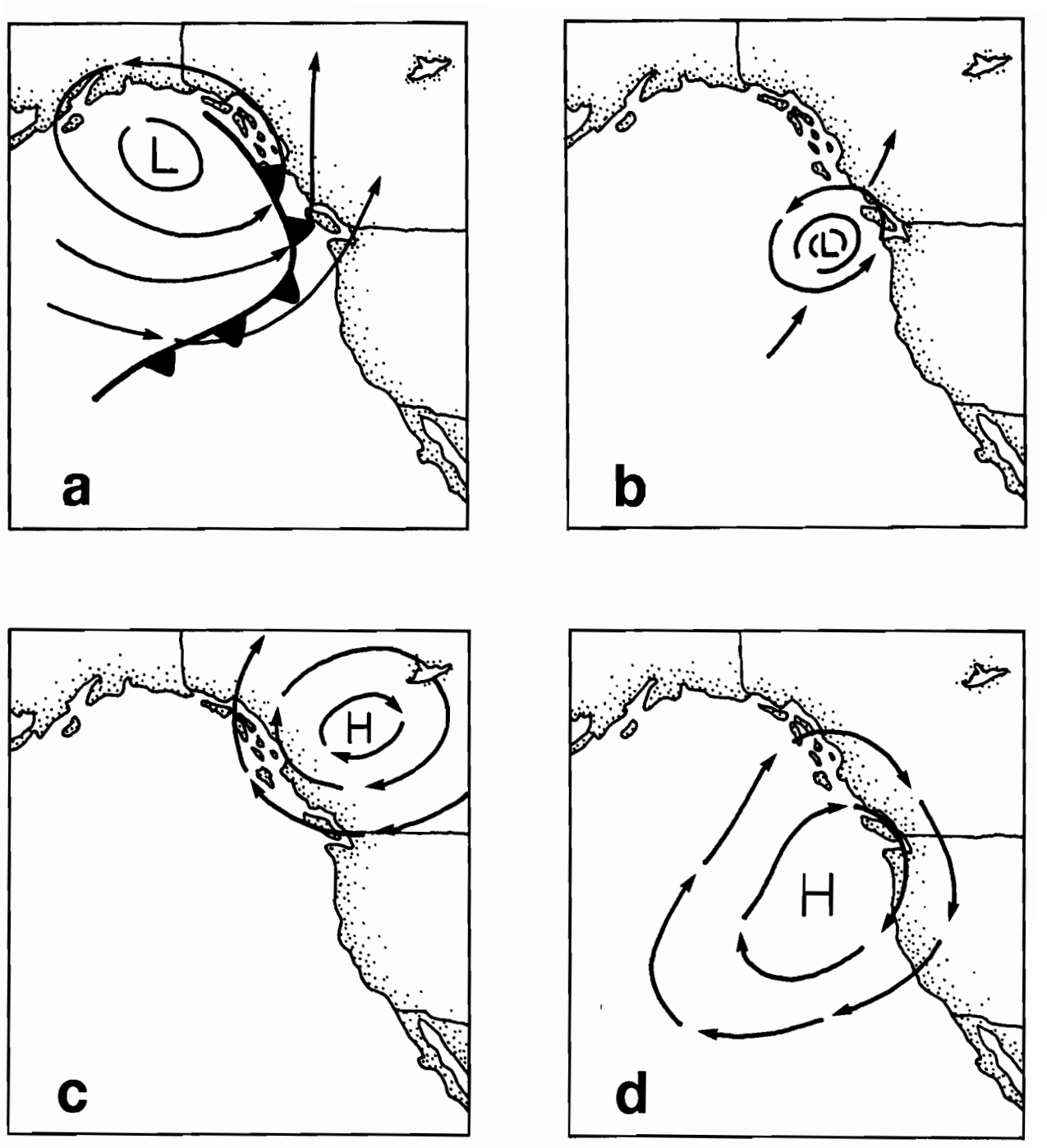

Figure 13. Typical weather patterns affecting the Pacific Northwest a) L1, b) L2, c) H1, d) H2 (Maunder, 1968; Overland, 1981).

In the second type of storm, L2 (Fig. 13b), small disturbances form in the central Pacific and move across the Pacific on a northeast trajectory, commonly passing parallel to the coastline or crossing over British Columbia. Such systems can rapidly intensify as they propagate north, seaward of the coastline, and produce some of the most severe Puget Sound weather, such as the Columbus Day storm in 1962 (Lynott and Cramer, 1966). A subset of this type is small synoptic-scale cyclones or "vortices" that form in the western Pacific behind major frontal bands such as L1 (Reed, 1979; Mullen, 1979; Locatelli et al., 1982).

At some time during most winters an upper-level blocking ridge of high pressure will develop over northwest Canada, accompanied by high pressure over the Puget Sound region, H1 (Fig. 13c). As a result, there are clear skies due to air mass subsidence induced by the high-pressure area, near-freezing temperatures, and very stable air in the surface layer of the atmosphere (Overland and Walter, 1981).

The summer season in Puget Sound is influenced by marine air from the Pacific moving over the region by way of the Strait of Juan de Fuca (Mass, 1982). From the end of June through August the synoptic situation is characterized by a marine high-pressure system influencing the area, H2 (Fig. 13d). This high-pressure influence leads to a dry season with many clear days, warm temperatures, and prevailing winds from the west to northwest. Cyclonic disturbances may still occur, but their severity is greatly lessened and their frequency is likewise diminished compared to winter.

The spring season is not significantly different from winter except that temperatures are higher due to increased insolation; the frequency of cyclonic disturbances decreases, and their distribution over time is irregular. The strength of the upper-level flow diminishes in intensity as spring progresses.

Autumn is another transition period. A common characteristic of early autumn is the continuing influence of the Pacific high-pressure system in the area. The high-pressure ridge eventually breaks down, shifting the prevailing winds to southwesterly and strengthening the upper-level flow. With this shift come the cyclones and fronts associated with winter.

The frequency of occurrence of these major map types is summarized by Table 6 derived from Maunder (1968). During winter months, December through February, lows predominate over highs by 3:1; type L1 forms 62% of the observed lows. By contrast, for the summer months, July through September, type H2 dominates on 48% of the days. Further discussion of typical synoptic weather situations for western Washington is given in Halladay (1970).

Table 6.--Number of days per month with synoptic weather patterns L1, L2, H1, H2*

Weather pattern	Month												
	J	F	M	A	M	J	J	A	S	O	N	D	YEAR
L1	14	10	7	12	7	4	5	5	5	14	10	13	106
L2	9	4	11	10	6	6	4	7	6	4	13	11	91
H1	4	2	3	0	1	1	1	1	3	6	3	4	29
H2	3	14	8	7	13	15	16	14	16	5	2	3	116

*Adapted from Maunder, 1968.

4. Regional Meteorological Phenomena

4.1. Overview

Regional weather phenomena are the result of the superposition of forcing on synoptic (1000 km), meso- (50 km), and local (5 km) scales. The interaction of synoptic-scale weather patterns and the topography of the region determines mesoscale and local meteorological features. For example, the Olympic Mountains affect wind and precipitation patterns because air mass stability confines airflow to the low-level marine channels, the N-S-oriented Cascade Mountains have a blocking effect on large-scale weather systems, and the proximity of the inland waters to the Pacific Ocean to the west and the highlands to the east of Puget Sound produces a strong diurnal variation of the summer wind pattern due to generation of land and sea breezes and valley winds.

The mountains restrict the free movement of air at sea level, which prevents geostrophic adjustment between pressure and wind, so that the earth's rotation has little effect on the direction of the wind; winds blow predominantly from high- to low-pressure in a direction dictated by the orientation of the low-level channels. Since Puget Sound is oriented at approximately a right angle to the Strait of Juan de Fuca, high pressure to the east gives easterly (i.e., down-gradient) winds in the Strait of Juan de Fuca and light winds in Puget Sound, while low pressure to the north gives strong southerly winds in Puget Sound and light winds in the central part of the Strait of Juan de Fuca. Wind speed (in knots) for the Strait of Juan de Fuca is roughly ten times the difference in the sea-level pressure (in millibars) at Bellingham and Quillayute; the wind speed for Puget Sound is roughly ten times the difference in pressure at Olympia and Bellingham (R. Anderson, personal communication; Overland, 1981).

Because of the different orientation of Puget Sound and the Strait of Juan de Fuca, a frontal passage can lead to differing time sequences of winds in the two regions (Church, 1938). For a typical example (Fig. 14), at 0500 Pacific Daylight Time (PDT), the lowest sea-level pressure is at the coast, which creates east winds in the Strait of Juan de Fuca. By 1100 PDT, the front has passed over the inland waters, and pressures are beginning to increase to the south behind the front giving rise to southerly winds in Puget Sound. By 1700 PDT, the front has passed to the northeast of Bellingham, and pressures have increased at the coast reversing the wind direction to westerly in the Strait of Juan de Fuca. Thus, the winds in Puget Sound have increased and then decreased from the south during the frontal passage, while the wind direction in the Strait of Juan de Fuca has reversed from east to west.

The following sections review studies that have recently led to a considerable increase in understanding of the factors affecting the meteorology of the Puget Sound region.

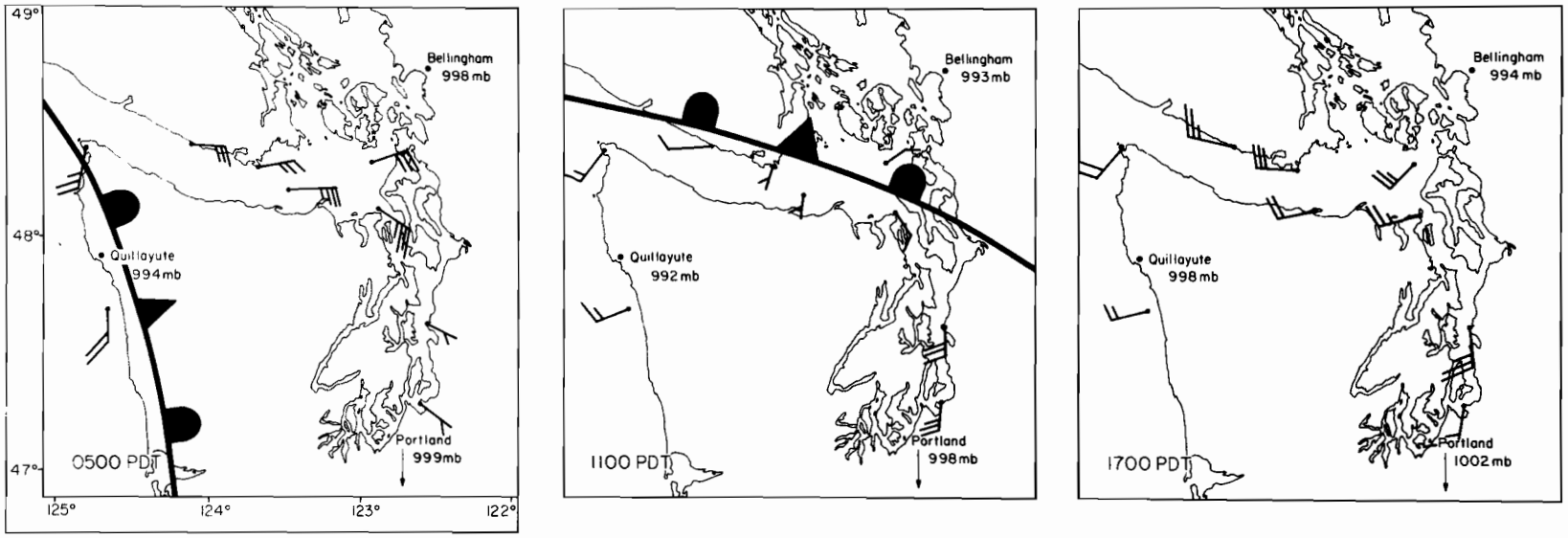

Figure 14. Typical local wind patterns for the passage of a front through western Washington (Overland, 1981).

4.2. Gap winds and bora

Several times during most winters a cold high-pressure area is established east of the Cascade Mountains with a low-pressure system offshore (Fig. 15a). This situation results in a large east-west pressure gradient over the Puget Sound region and the formation of locally strong and at times destructive winds. Reed (1931) applied the term "gap winds" to the strong easterly winds observed in the Strait of Juan de Fuca under these conditions and characterized these winds as "not being, properly speaking, gradient winds in that geostrophically balanced pressure gradients are totally inadequate alone to account for the velocities observed." He defined "gap winds" as the flow of relatively homogeneous air in a sea-level channel with a source region or reservoir at one end. A component of the pressure gradient parallel to the channel causes the flow to accelerate along the channel. Reed also concluded that the high velocities in the Strait of Juan de Fuca were due to a venturi effect caused by the converging sides of the channel.

In a more recent investigation of gap wind conditions, Overland and Walter (1981) combined high-resolution, low-level (50-m) wind fields derived from aircraft flights over the Straits of Juan de Fuca and Georgia with surface data and upper-air soundings. It was found that the presence of converging sides of the channel was incidental to the increased wind speeds and that acceleration due to the pressure gradient along the channel alone was sufficient to explain the observed wind magnitudes. An example for the period 2040-2400 GMT 23 February 1980 is shown in Fig. 15b. Winds in the Strait of Georgia were light and variable where the pressure gradient was flat; in the eastern part of the Strait of Juan de Fuca the flow was generally disorganized but tended to have an easterly component. In the central and western portion of the Strait of Juan de Fuca the component of the pressure gradient along the axis of the channel remained nearly uniform, while the winds increased to 14 m s^{-1} at the entrance to the Strait. Vertical wind speed measurements from the aircraft indicated that subsidence was occurring over the inner part of the Strait of Juan de Fuca and the Strait of Georgia, whereas vertical motion was upward west of 124°20'W.

For the inland waters of Puget Sound and the Strait of Juan de Fuca, the acceleration of the wind provides the primary balance to the component of the sea-level pressure-gradient force imposed by the synoptic weather situation along the direction of the various channels. For flow at constant height the increase in wind speed due to a constant sea-level pressure gradient is given by the Bernoulli equation:

$$\frac{u^2}{2} = \frac{u_o^2}{2} - \frac{\Delta p}{\rho} , \qquad (1)$$

where u is velocity, u_o is an initial velocity, Δp is the pressure difference, and ρ is a density.

A situation similar to 23 February occurred on 13 February 1980, but in this case the major pressure gradient was situated over southern British Columbia (Fig. 16a). The pressure gradient accelerated the cold, dry continental air from the interior of British Columbia through the Fraser River

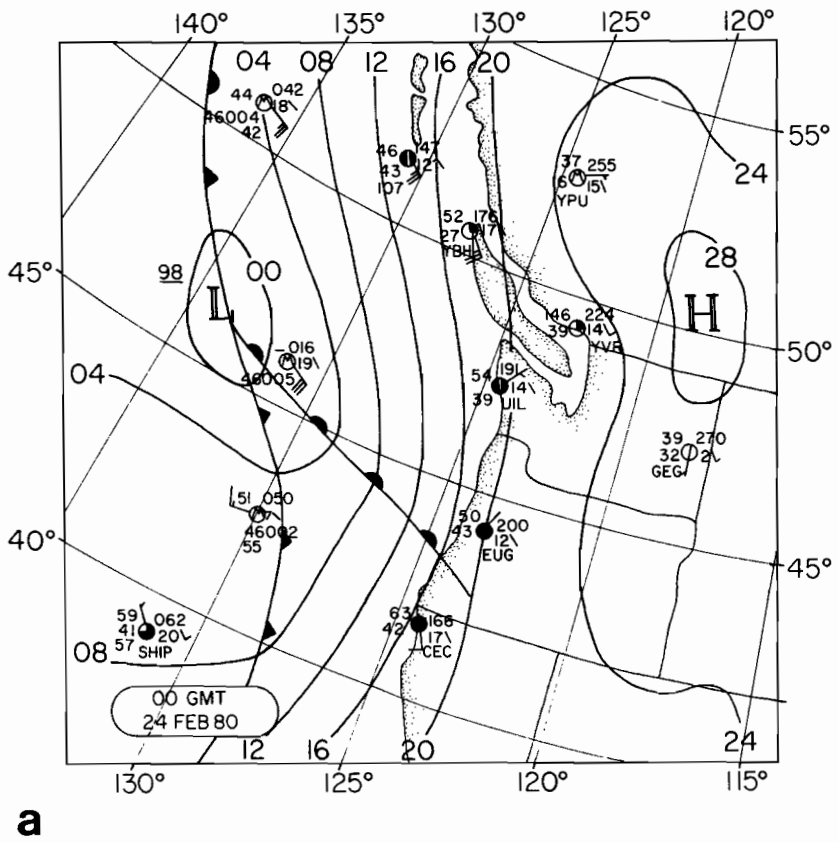

a

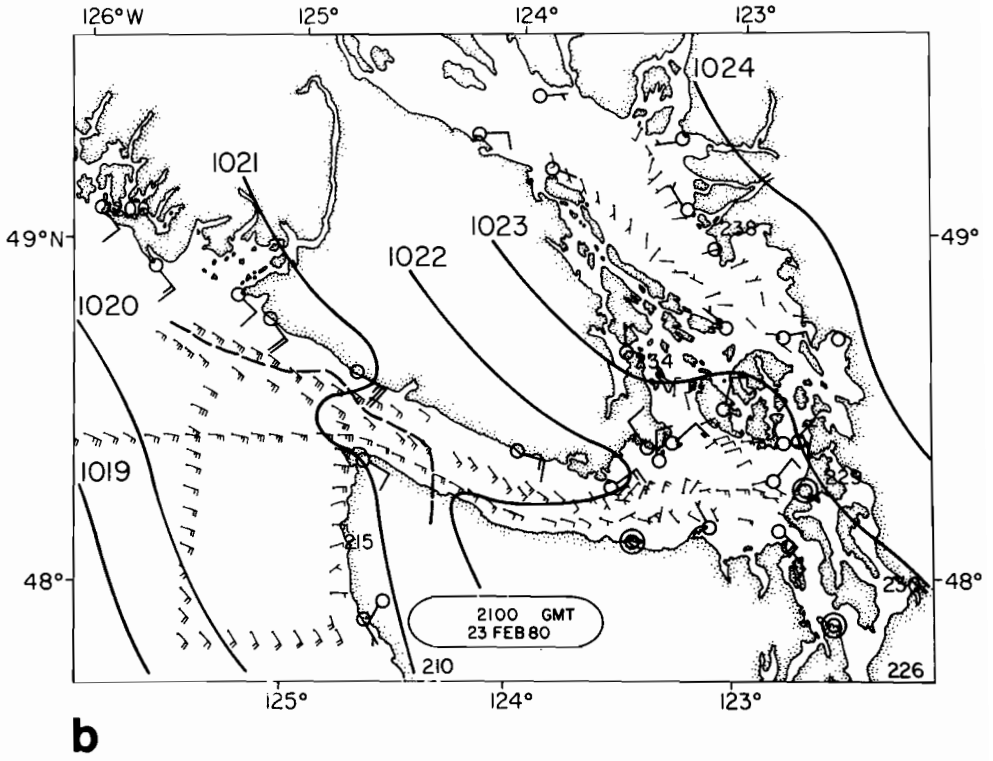

b

Figure 15. (a) Sea-level pressure analysis for 00 GMT 24 February 1980 for western Washington (Overland and Walter, 1981).

15. (b) Local wind field on 23 February and sea-level pressure analysis for 21 GMT 23 February 1980 for the Straits of Juan de Fuca and Georgia (Overland and Walter, 1981). Flight level wind measurements are shown as small wind arrows. Bold arrows with circles indicate surface station or buoy reports. Wind convention is in knots. The heavy dashed line at the entrance to the Strait of Juan de Fuca represents a transition from subsidence on the north and east side to positive vertical motion seaward of the line.

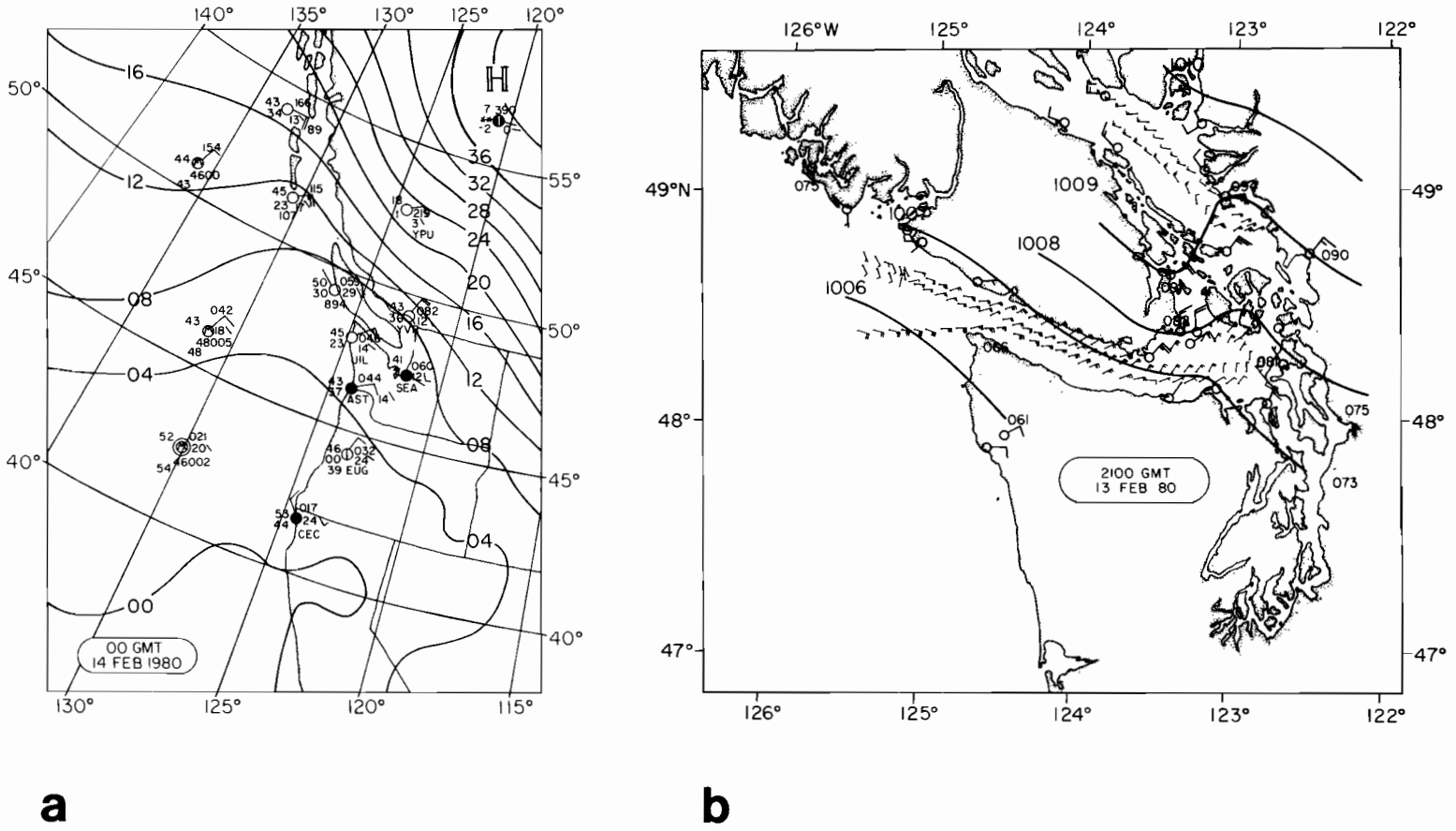

a b

Figure 16. (a) Sea-level pressure analysis for 00 GMT 14 February 1980 (Overland and Walter, 1981). (b) Local wind field on 13 February 1980 and sea-level pressure analysis for 21 GMT 13 February 1980 (Overland and Walter, 1981).

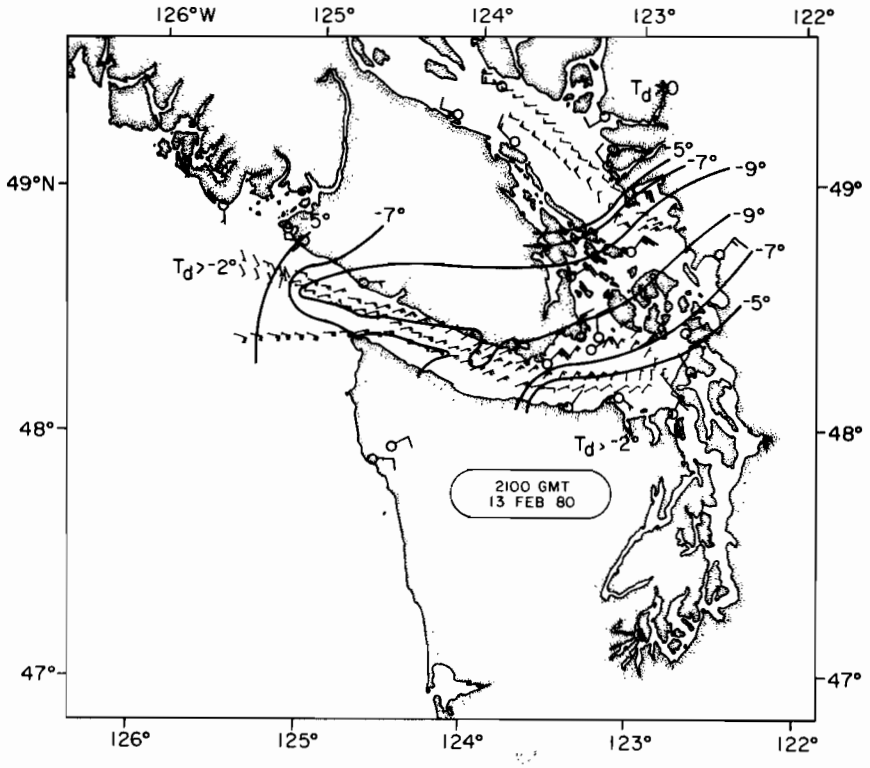

c

Figure 16. (c) Wind and dewpoint fields from surface and aircraft reports 21-24 GMT 13 February 1980 (Overland and Walter, 1981).

Valley near Vancouver (Fig. 16b). This dry air displaced the more moist, marine air as it flowed across Georgia Strait and was ultimately channelled out the Strait of Juan de Fuca (Faulkner, 1980). The change of dewpoint temperature marked the air mass boundaries (Fig. 16c). The dry air maintained an essentially constant velocity while spreading laterally and growing in depth, as shown by a downstream increase in inversion height. The momentum contained in the jet increased with downstream distance due to the presence of a pressure gradient along the flow direction. The eddy-like feature beyond the entrance to the Strait of Juan de Fuca, which had light SE winds to the west of its boundary and strong (10-12 m s^{-1}) winds from the E to the east of the boundary, may have been due to the presence of a hydraulic jump. Vertical wind speeds as recorded by the aircraft were downward at 1 m s^{-1} on the east side and upward at 0.4 m s^{-1} on the west side of the boundary.

Another response of the flow in Puget Sound to pressure differences is the creation of a downslope wind called a bora, which blows out of the passes in the Cascade Range when high pressure exists to the east of the mountains. Since the source region for the air in eastern Washington is often very cold, the adiabatic heating of the air upon descent out of the passes is not sufficient to raise the temperature to levels equal to ambient conditions in the Puget Sound Basin, so the cold air spreads out over the lowlands. Reed (1981) discussed a windstorm that led to a bora-like flow in Stampede Pass and gap winds in the Columbia River Gorge. Figure 17 shows the extremely large gradient of sea-level pressure in the vicinity of the Cascades for 28 November 1979. This gradient was for the most part fictitious, merely indicating that the mountain barrier sustained a large pressure difference between the cold air in central and eastern Washington and the warm air over western Washington. An E-W cross section (Fig. 18) of potential temperature across the State of Washington from Spokane (GEG) to Quillayute (UIL) showed the intense horizontal temperature gradient that developed over and to the lee of the mountains as the upper-level inversion tilted and lowered in the subsiding airflow. Rewriting (1) using pressure coordinates gives:

$$\frac{u^2}{2} = \frac{u_0^2}{2} - g \frac{\partial \bar{D}}{\partial x} \Delta x \ , \qquad (2)$$

where g is gravity, D is the geopotential height deviation from the standard value for a particular pressure level and Δx is the difference in horizontal distance between the end points of the trajectory. Calculations using Eq. (1) in the Columbia River Gorge and Eq. (2) for flow in the lee of Stampede Pass estimated sufficient wind magnitudes to account for those observed.

4.3. Orographic low-pressure formation in the lee of the Olympic Mountains

During the winter (December-February), synoptic weather patterns give rise to S-SW flow conditions over the Puget Sound region 75% of the time. When synoptic-scale winds are from the south-to-southwest, the Olympic Mountains can induce the formation of a low-pressure area directly in the lee of the mountains over Puget Sound or the Strait of Juan de Fuca (Overland et al., 1979), and Vancouver Island can induce low pressures over the Strait of

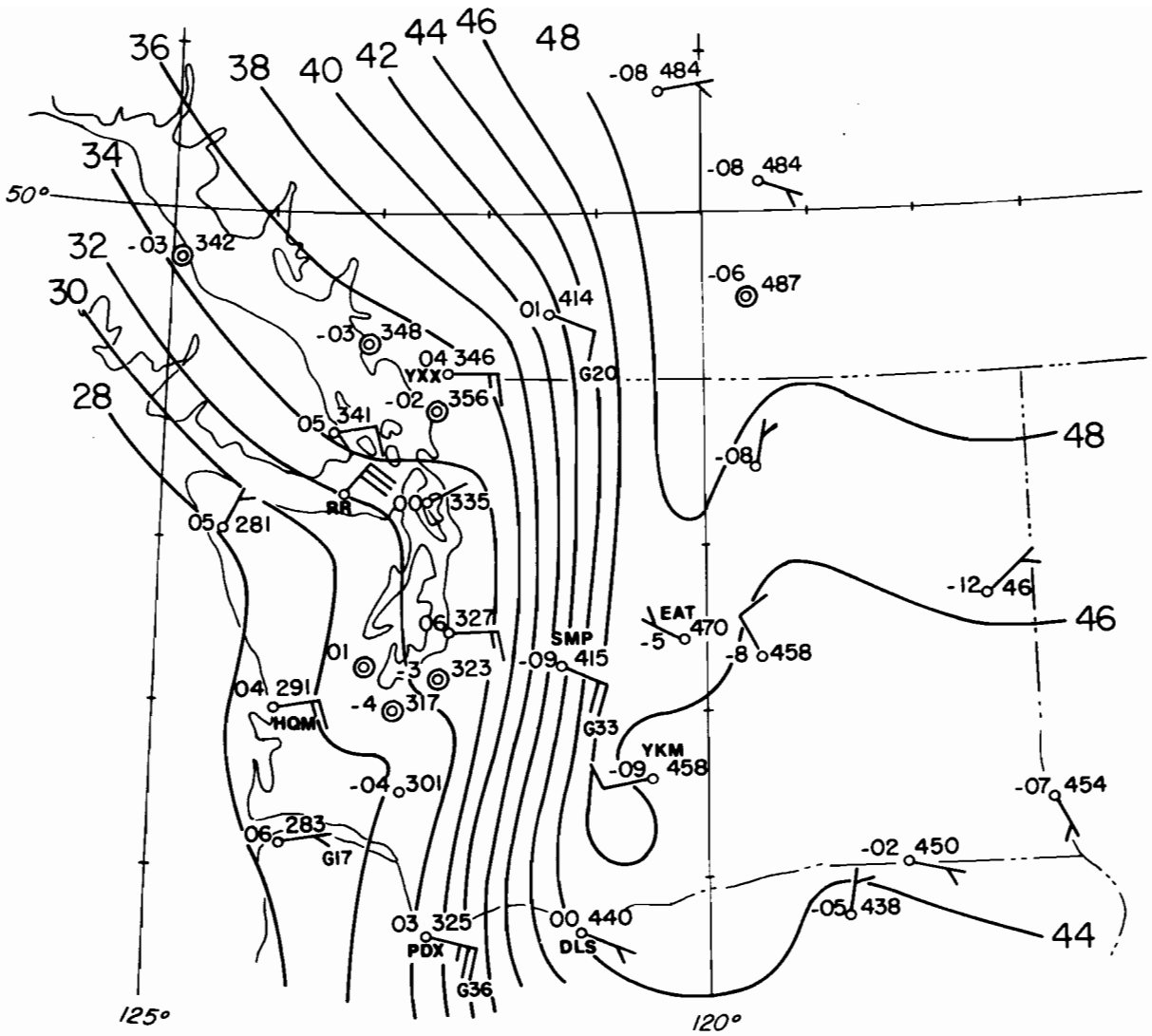

Figure 17. Surface map, 12 GMT 28 November 1979. Isobars are drawn at intervals of 2 mb. Temperature (°C) is plotted to left of station and pressure (mb) to right of station (Reed, 1981).

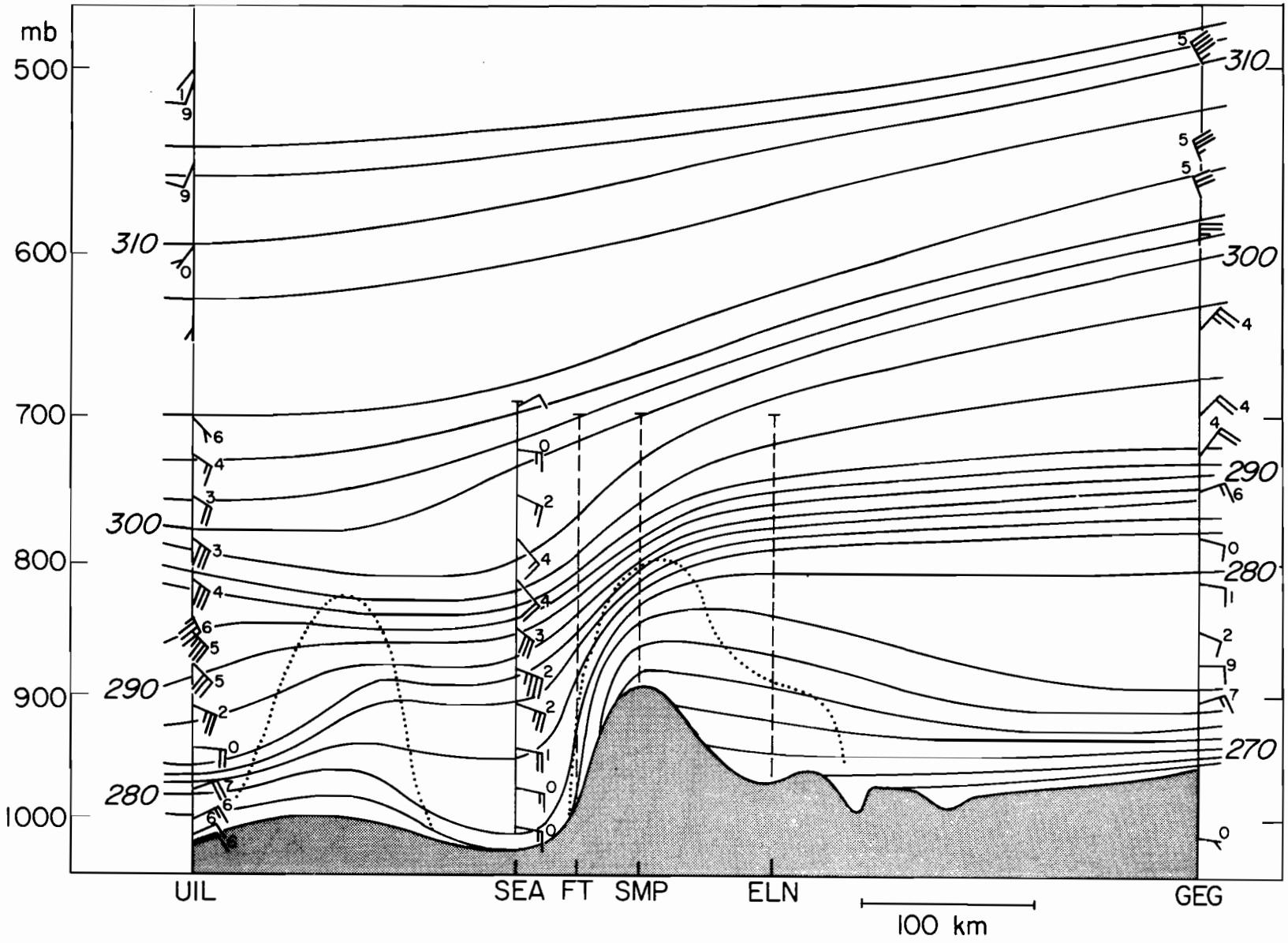

Figure 18. Cross section of potential temperature (°K) across the state of Washington (Reed, 1981). Station UIL is Quillayute, SEA is Seattle, and GEG is Spokane.

Georgia (Myers, 1966). The importance of the presence of such a low-pressure area was dramatically demonstrated on 13 February 1979 when the Hood Canal Bridge sank during surface winds in excess of 50 m s^{-1}. Reed (1980), who analyzed the meteorological conditions for this event, found that although the gradient of sea-level pressure at the bridge was strong due to the synoptic pressure gradient, it was greatly enhanced by the formation of a mesoscale low-pressure area in the lee of the Olympics (Fig. 19). In the restricted channels of Puget Sound the air flow at the surface accelerated toward the low pressure producing the observed high wind speeds. In contrast, Walter and Overland (1982) made measurements with the NOAA P-3 aircraft on three days during S-SW conditions in February and March 1980 (Fig. 20a-f) and found a region of light wind speed and flat pressure gradient in the lee of the Olympic Mountains and only slight troughing in the pressure field over the eastern Strait of Juan de Fuca.

To explain this difference one needs to consider a non-dimensional number, the internal Froude number, F, which compares the momentum of the incident flow to the stratification of the flow. This number is the critical parameter in determining whether the upstream air will go over (large F) or around (small F) an isolated obstacle such as the Olympic Mountains. For a fluid having continuous stratification the Froude number is given by

$$F = \frac{V}{hN_e}, \qquad (3)$$

where V is upstream flow velocity, h is the height of the mountain, and N_e is the stratification parameter, the Brünt-Väisälä frequency,

$$N_e^2 = \frac{g}{\theta_e} \frac{d\theta_e}{dz}, \qquad (4)$$

where g is gravity, θ_e is the equivalent potential temperature, and z is the vertical coordinate. The vertical derivative of equivalent potential temperature accounts for stratification due to moisture as well as ambient temperature. On the three days discussed by Walter and Overland (1982), the boundary layer was slightly stable throughout its depth with the internal Froude number in the range F = 1.0-1.4. For the Hood Canal Bridge storm a smaller value of N_e together with high upstream winds led to a calculated value for F of 4.6.

For strong relative stratification, the primary flow about an obstacle is in quasi-horizontal planes (Fig. 21a and b) where the flow in each plane is given by a two-dimensional potential solution defined by the contour of the terrain at that level (Drazin, 1961; Riley et al., 1976; Hunt and Snyder, 1980). Small vertical displacements of the streamlines passing around the side of the obstacle are due to the need for the potential energy to decrease in order to balance the increase in kinetic energy of the flow around the obstacle. Although the Froude numbers for the low wind studies in Walter and Overland (1982) were in the range of 1.0-1.4, the pressure and wind fields (Figs. 20 b,d,f) show qualitative agreement with experimental results for

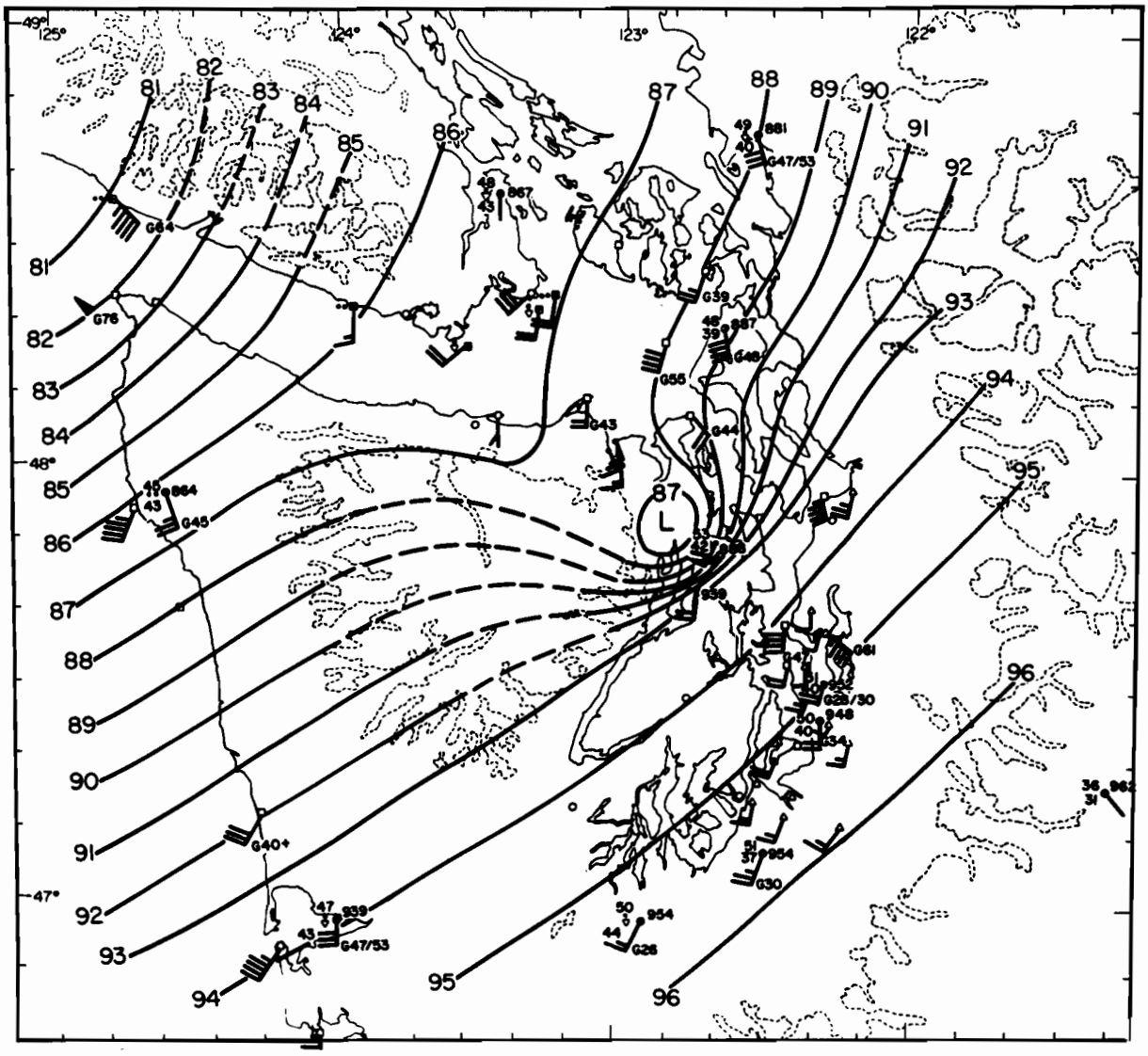

Figure 19. Regional surface map for 12 GMT 13 February 1979 (after Reed, 1980). Isobars are drawn at one millibar intervals (dashed at higher elevations). Winds are in knots. Maximum gusts (G) at observation time and in preceding hour are plotted below stations.

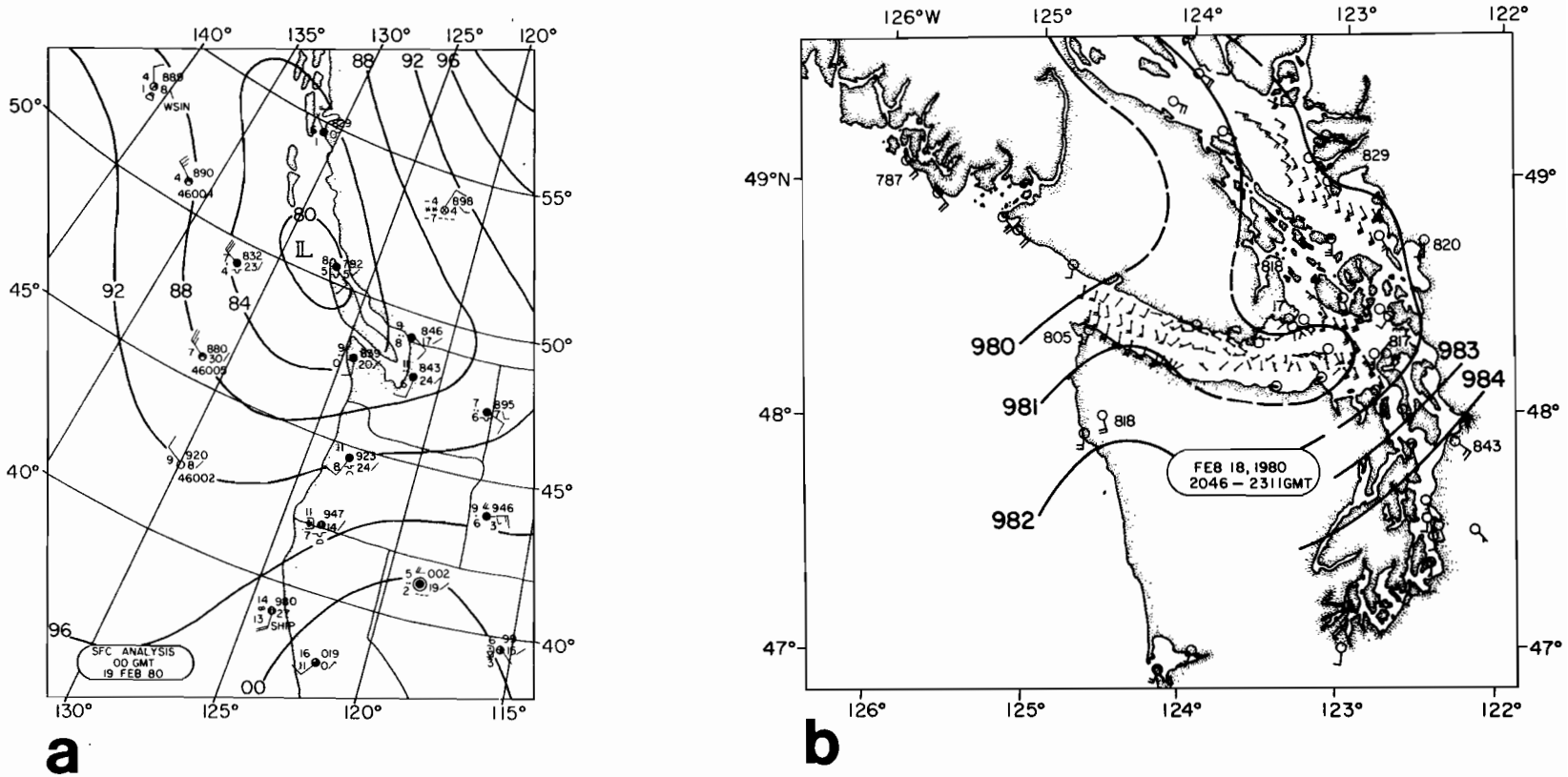

Fig. 20. (a) Sea-level pressure analysis for 00 GMT 19 February 1980 and (b) mesoscale wind and pressure field at 21 GMT 18 February 1980.

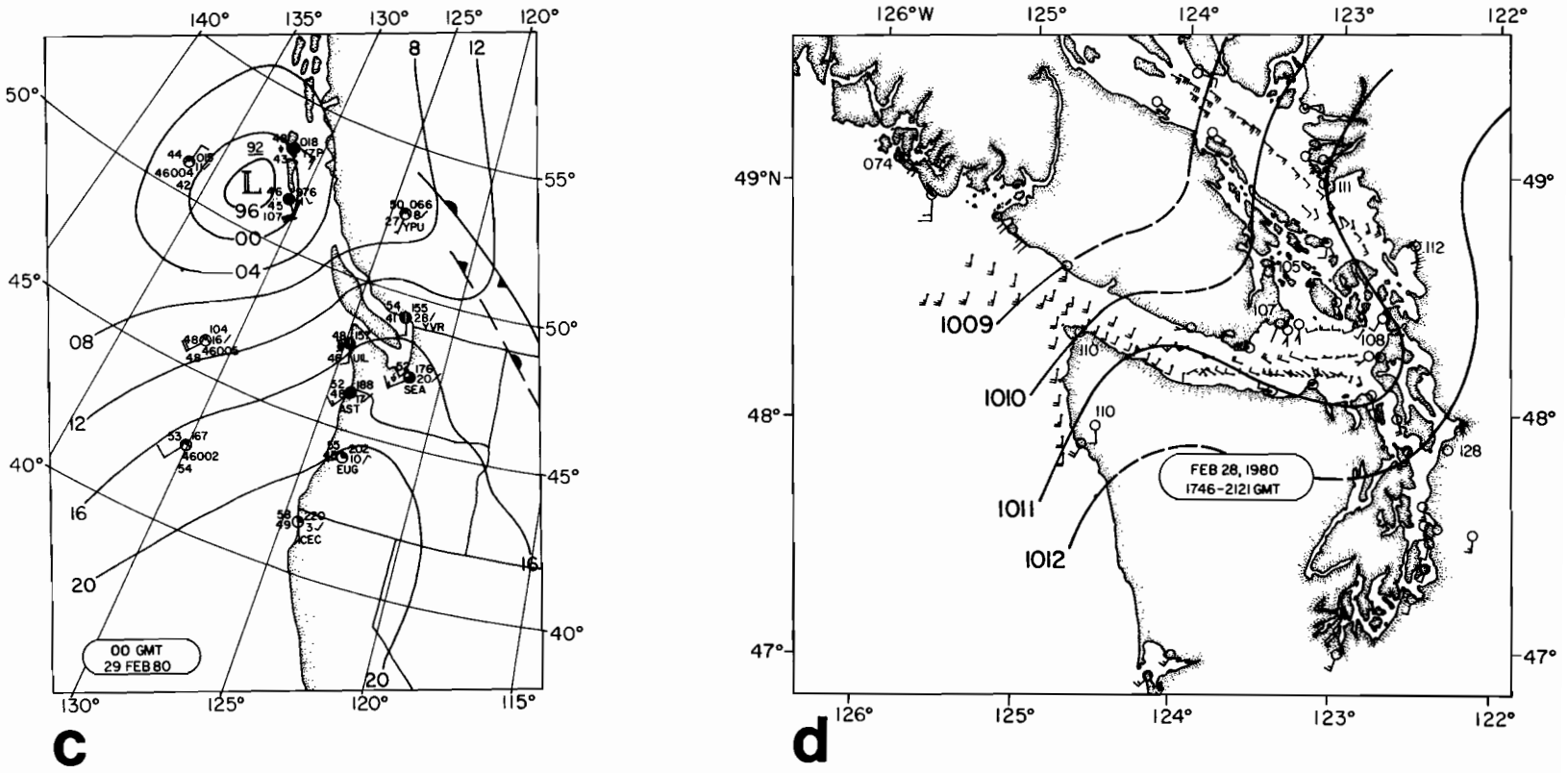

Fig. 20. (c) Sea-level pressure analysis at 00 GMT 29 February 1980 and (d) mesoscale wind and pressure field at 21 GMT 28 February 1980.

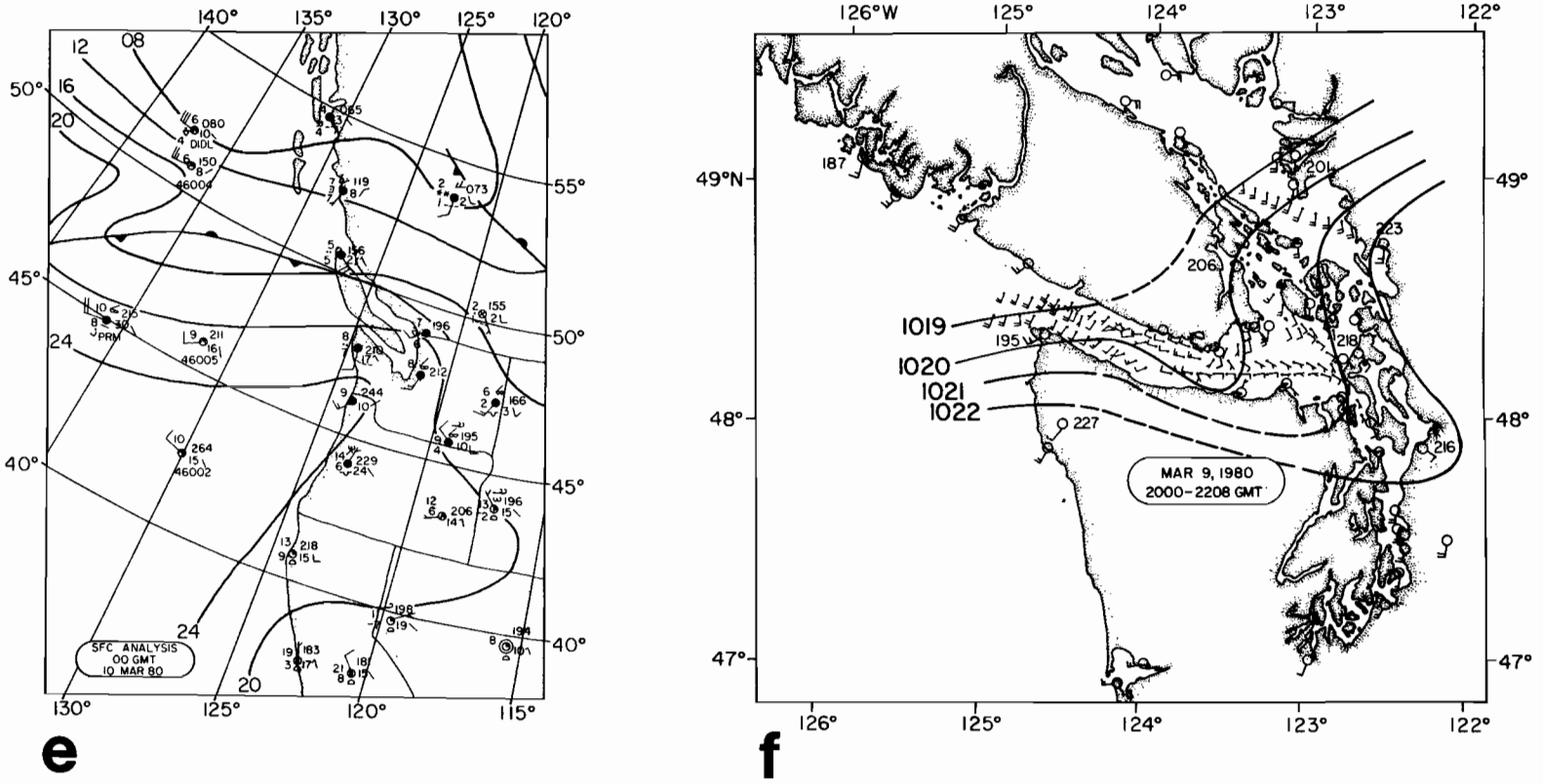

Figure 20. (e) Sea-level pressure analysis at 00 GMT 10 March 1980 and (f) mesoscale wind and pressure field at 21 GMT 9 March 1980.

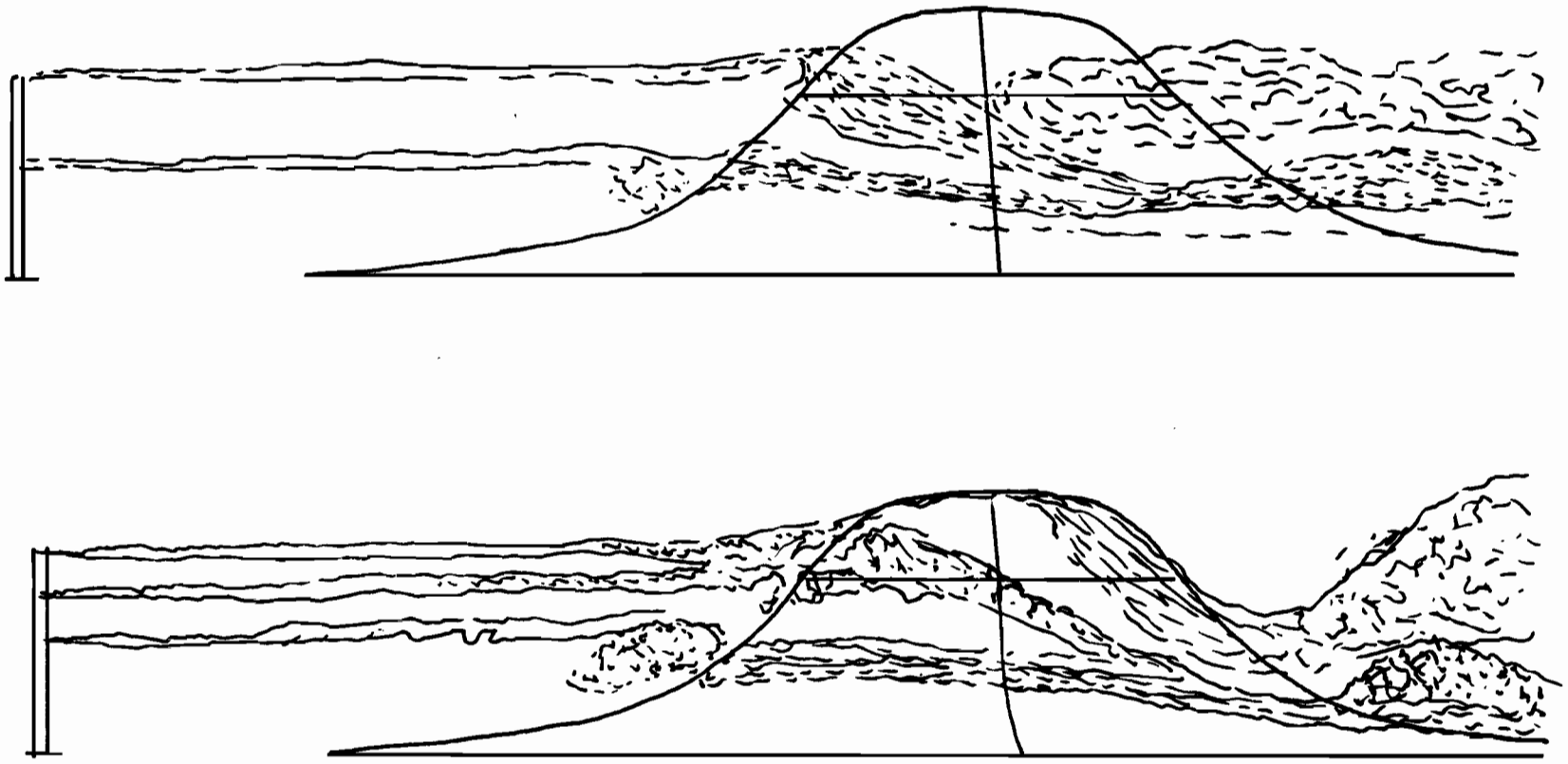

Figure 21a. Plumes from upwind stacks at various elevations (Hunt and Snyder, 1980). Top is for F = 0.2. Flow is constrained to move principally in horizontal planes. A slight hydraulic jump occurs just downstream from the top of the hill. Bottom is for F = 0.4. Here the flow is able to move farther in the vertical direction, and the region where the flow goes over the top is broader. Flow going over the top separates half-way down the lee slope.

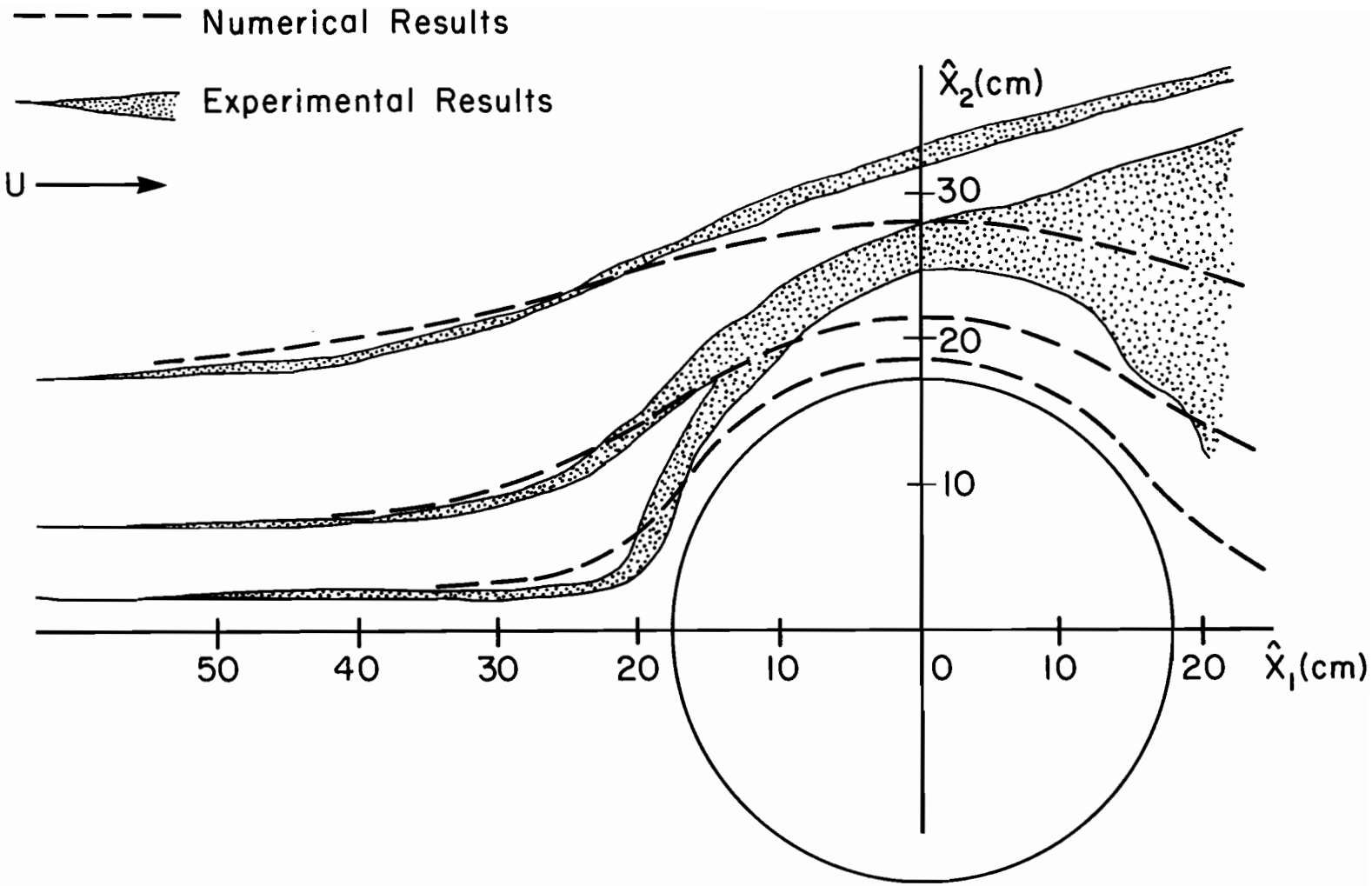

Figure 21b. Comparison of experimental and analytically computed (Drazin, 1961), streaklines in the horizontal plane at mid-level of a Gaussian-shaped obstacle for a Froude number of 0.154 (Riley et al., 1976).

low Froude number flow. However, from the magnitude of the isotherm displacement in cross-section plots of constant θ surfaces along the east side and in the lee of the Olympics, it was evident that the flow was approaching the transition region between small and large Froude number theory.

For the case where F >> 1, Smith (1980) developed a hydrostatic linear model for stratified flow over an isolated mountain. His results for a bell-shaped mountain showed an asymmetric perturbation surface pressure field with high pressure over the windward slope and low pressure on the lee side. This pressure distribution caused the surface streamlines to be deflected around the sides of the mountain and to maintain a permanent outward deflection downstream. Horizontal divergence in the lee of the mountain caused a sinking of warm air from aloft and a decrease in the vertical distances between downwind, low-level, constant-density surfaces. When this perturbation pressure field is added to the background synoptic-scale pressure field (Smith, 1981; Fig. 22), the result is in agreement with the sea-level pressure analysis for parameters from the Hood Canal storm (Fig. 19).

Reed (1980) indicated that in the vicinity of the Hood Canal Bridge on 13 February 1979 the pressure gradient was a maximum of 6 mb in 15 km or 0.4 mb km^{-1}. Comparison of the observed winds at the time of the bridge collapse (from Reed, 1980, Table 2) with those calculated for a confined channel from Eq. (1) and a value of the pressure gradient of 0.4 mb km^{-1} shows good agreement (Table 7).

When the internal Froude number has a value on the order of 0.5-1.5, the flow response in the lee of the Olympics will be relatively benign with light and variable winds. However, when the Froude number is of order 4-5, a closed mesoscale low-pressure region will be induced in the lee of the mountains. The flow at the surface in the restricted channels of Puget Sound responds by a rapid acceleration toward low pressure to give extreme wind speeds in a localized area.

4.4. Effects of orography on precipitation--the Puget Sound convergence zone

The surrounding mountains not only have a strong effect on the wind fields but also on the precipitation patterns in Puget Sound as shown by Mass (1981) and Parsons and Hobbs (1982). In the spring transition months (April-June), when high pressure builds northward into the eastern Pacific Ocean, the coastal winds change from a predominantly southerly to a northwesterly direction. As southerly winds veer to the northwest after a frontal passage at the coast, there is a narrow range of wind directions and speeds (Fig. 23) where the air will simultaneously flow eastward both north and south of the Olympic Mountains. This flow pattern results in the formation of an area of convergence over Puget Sound (Fig. 24). Mass (1981) studied 25 cases of this convergence phenomenon and concluded that the controlling parameters were the wind direction and speed on the Washington coast, although most convergence zone events were also associated with weak atmospheric stability typical of spring. He found that a convergence event was most likely to occur when, for four continuous hours, the Hoquiam wind direction was between 260° and 320° and the wind speed ranged from 2 to 7 m s^{-1}. Although convergence events can occur any time of the year, they are most probable from April to June when two to four major events per month are expected.

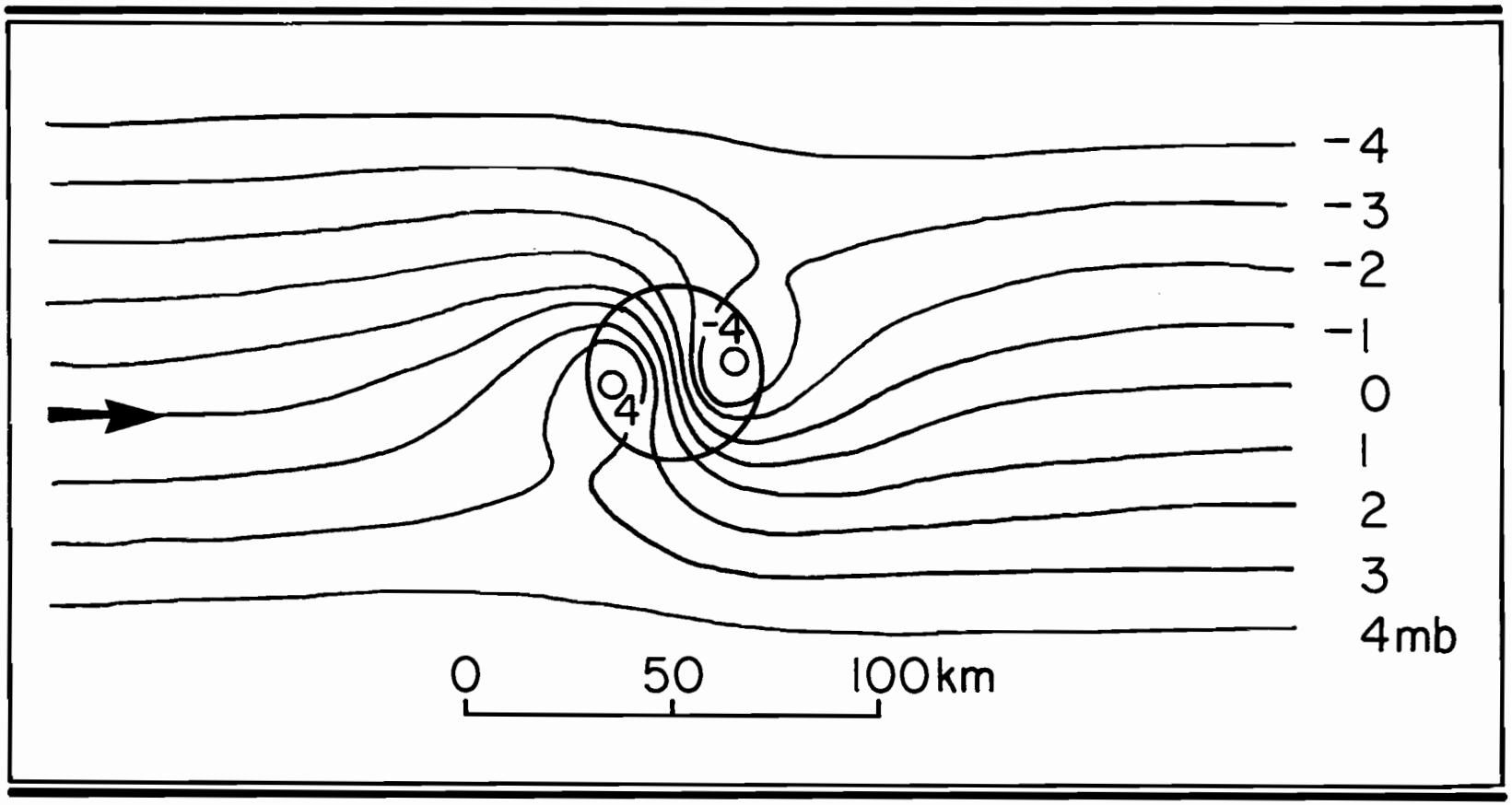

Figure 22. Sum of the perturbation pressure field from Smith's hydrostatic linear model and a hypothetical synoptic pressure field (Smith, 1981).

Table 7.--Comparison of winds reported by Reed (1980) in Hood Canal 14-15 GMT 13 February 1979 and those calculated from Eq.1*

	Observed	Calculated
Bridge	40 m s^{-1}	40.5 m s^{-1}
9.25 km SSW	30	33
18.5 km SSW	22.5	22.5 (assumed)

*Initial velocity used for the calculation is 22.5 m s^{-1}.

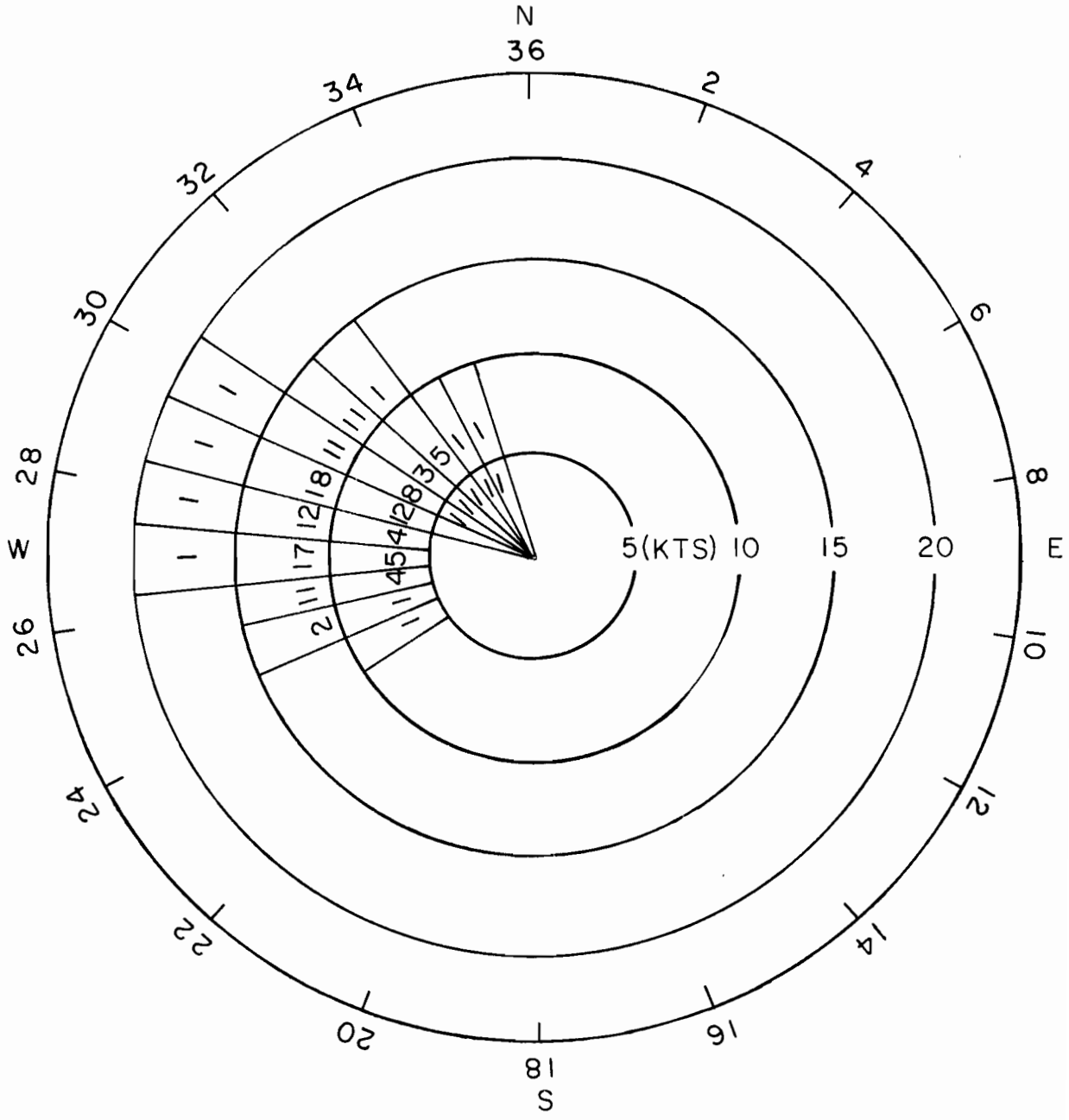

Figure 23. Polar representation of the wind speed and direction at Hoquiam, Washington, during ten convergence zone events (Mass, 1981).

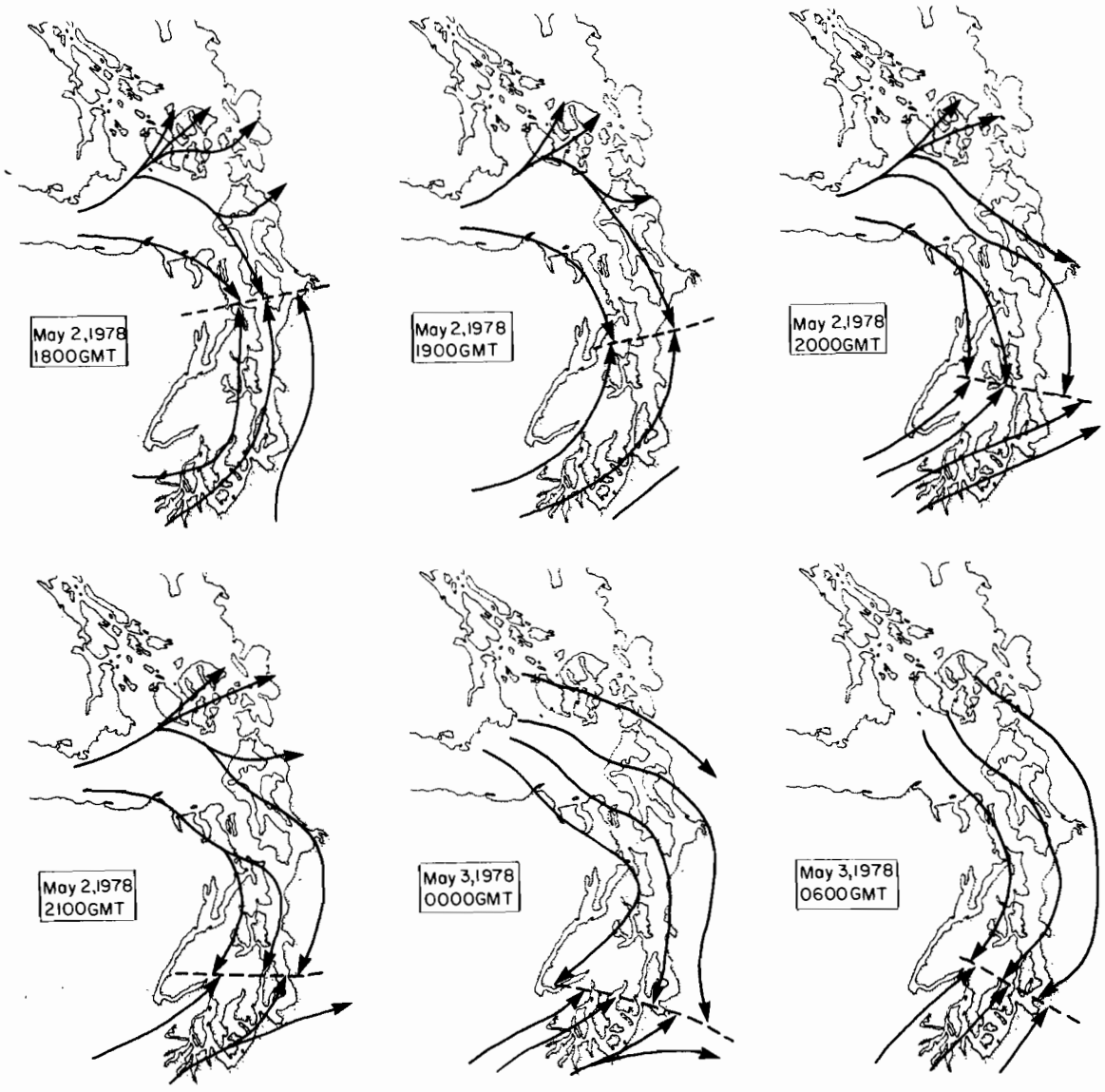

Figure 24. Streamlines over the Puget Sound area during the convergence zone event of May 2-3, 1978 (Mass, 1981). The position of the surface convergence line is indicated by a dashed line.

A composite vertical structure of the convergence zone was constructed by Mass (1981), who indicated that it is similar to that of a classical front. Northerly winds enter Puget Sound and propagate as a wedge into the pre-existing southerly winds (Fig. 25). The windshift line separating the opposing flows slopes upward to the north. Enhanced clearing is observed both north and south of the main convergence zone cloud band. Mass (1981) indicated that the clear area north of the zone is due to subsidence associated with the surface divergence created as air flow in the eastern Strait of Juan de Fuca splits and moves both north into the Strait of Georgia and south into Puget Sound. The clear region to the south of the zone is due to subsidence of air in the mesoscale circulation set up above the convergence line.

The presence of the convergence zone has pronounced effects on the cloudiness, temperature, and precipitation patterns over the region, and its effects can be seen in Figures 26 a-c, which are composites of these parameters for the cases studied by Mass (1981) plotted with reference to the location of the convergence line. Most of these convergence events showed a band of clouds across central and northern Puget Sound with the southern boundary close to the windshift line. These clouds were generally shallow, with tops between 1500 and 2500 m in the central Sound and 3000 m near the mountains. The lowest cloud deck in the Sound frequently reached to the ground.

The effect of the convergence zone on precipitation can be seen in the long-term climatology. Mass (1981) constructed a N-S cross section of monthly precipitation for Puget Sound (Fig. 27). There is a normal annual cycle at all stations except in the northern Sound where there was sustained precipitation through May and June caused by convergence zone precipitation.

Parsons and Hobbs (1983) studied the effects of orographic features in the Puget Sound region on mesoscale structures and precipitation processes in different types of rainbands embedded in synoptic-scale storms as they pass across the region. They studied warm-frontal, warm-sector, narrow and wide cold-frontal, and post-frontal rainbands and found that the influence of orography was dependent on the rainband type, the size of the orographic feature, and the airflow. Figure 28 shows that a large percentage of precipitation from warm-sector (i.e., pre-frontal) rainbands occurs at three coastal stations due to slight lifting of the airmass and from post-frontal rainbands at three stations about 100 km inland, where precipitation is considerably enhanced over the windward slopes of the Cascades. Local airflow convergence caused by the restricted flow in channels of the Puget Sound Basin also played an important role in enhanced post-frontal precipitation.

4.5. Diurnal wind variations--the sea breeze and valley breeze

In the warm months of the year the wind field shows a strong diurnal variation that is related to differential heating between the land and adjacent waters and heating on the mountain slopes. Staley (1957) presents hodographs--plots of the rotation of wind vector end points with time of day (Fig. 29)--for July 1950, where resultant winds were derived by averaging components of the wind observed at each hour during the day over a month. In the Strait of Juan de Fuca, Port Angeles showed W-NW flow and counterclockwise rotation while Victoria showed southerly and southwesterly flow with clockwise rotation.

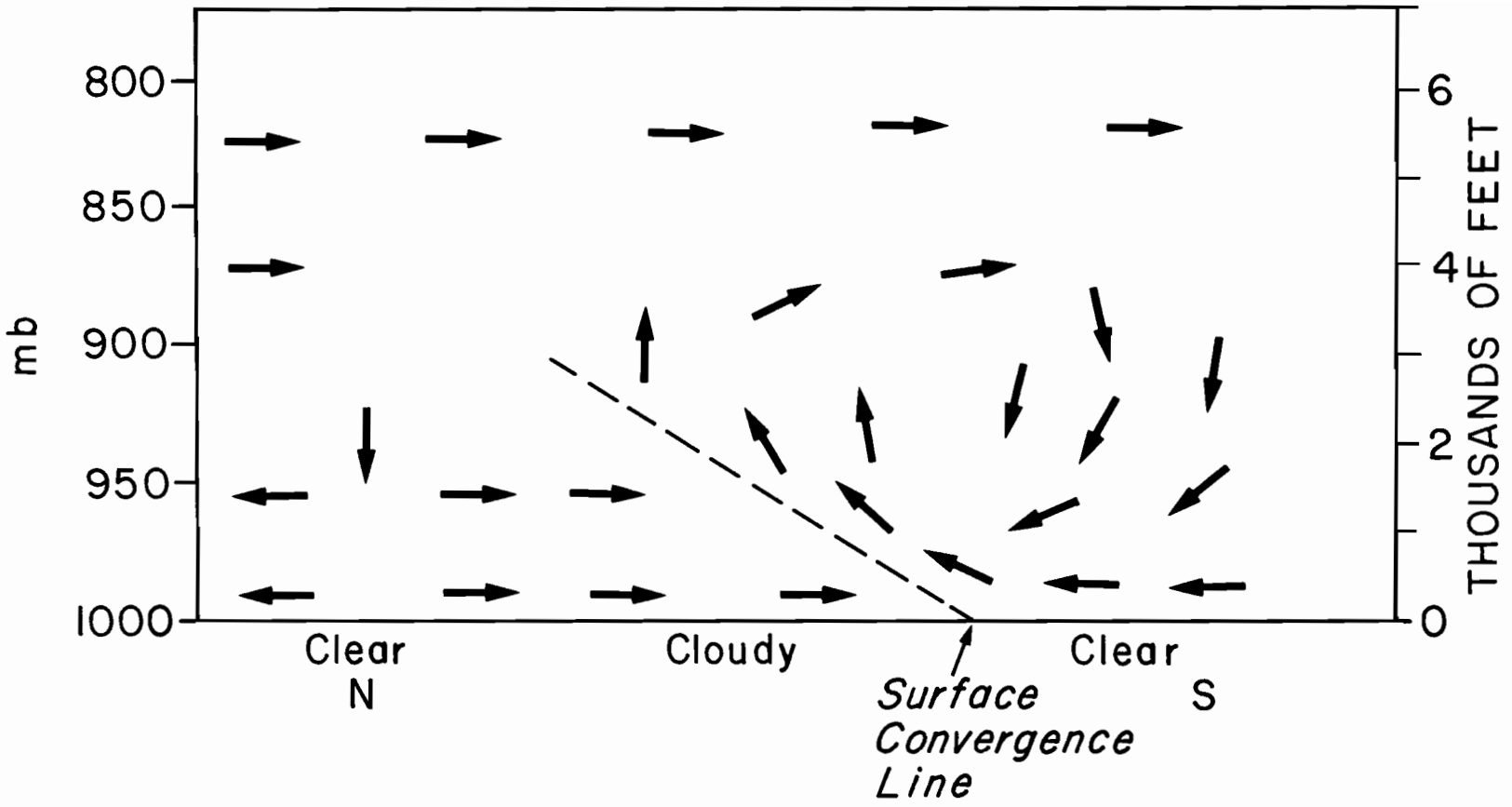

Figure 25. Schematic view of the low-level flow during a convergence event (Mass, 1981).

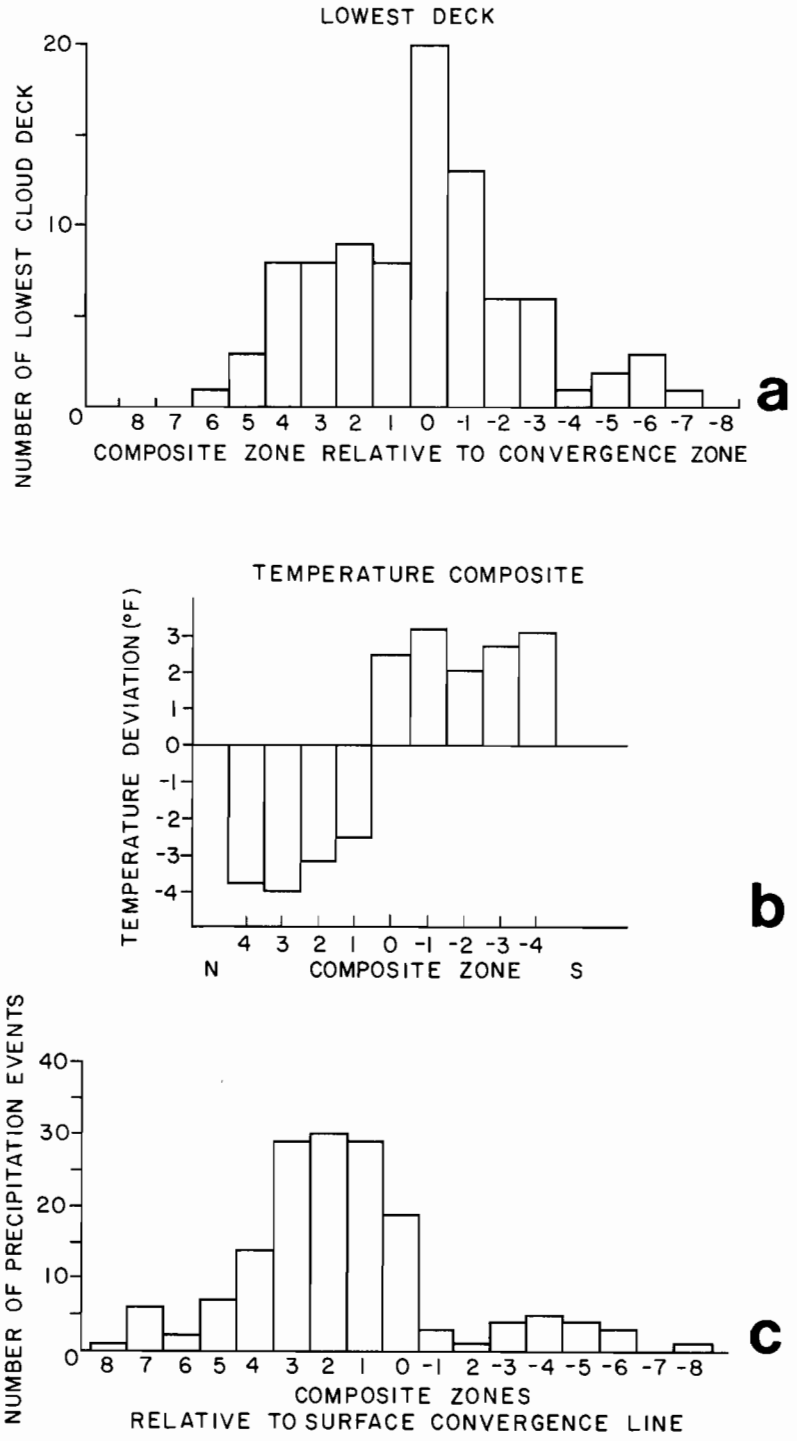

Figure 26. (a) Summary of the number of times the lowest cloud deck in Puget Sound occurred in each composite zone during five convergence zone events (Mass, 1981). (b) Temperature deviations (°F) from the Puget Sound mean for each composite zone (Mass, 1981). (c) Summary of the number of precipitation events that occurred in each composite zone during ten convergence zone events (Mass, 1981).

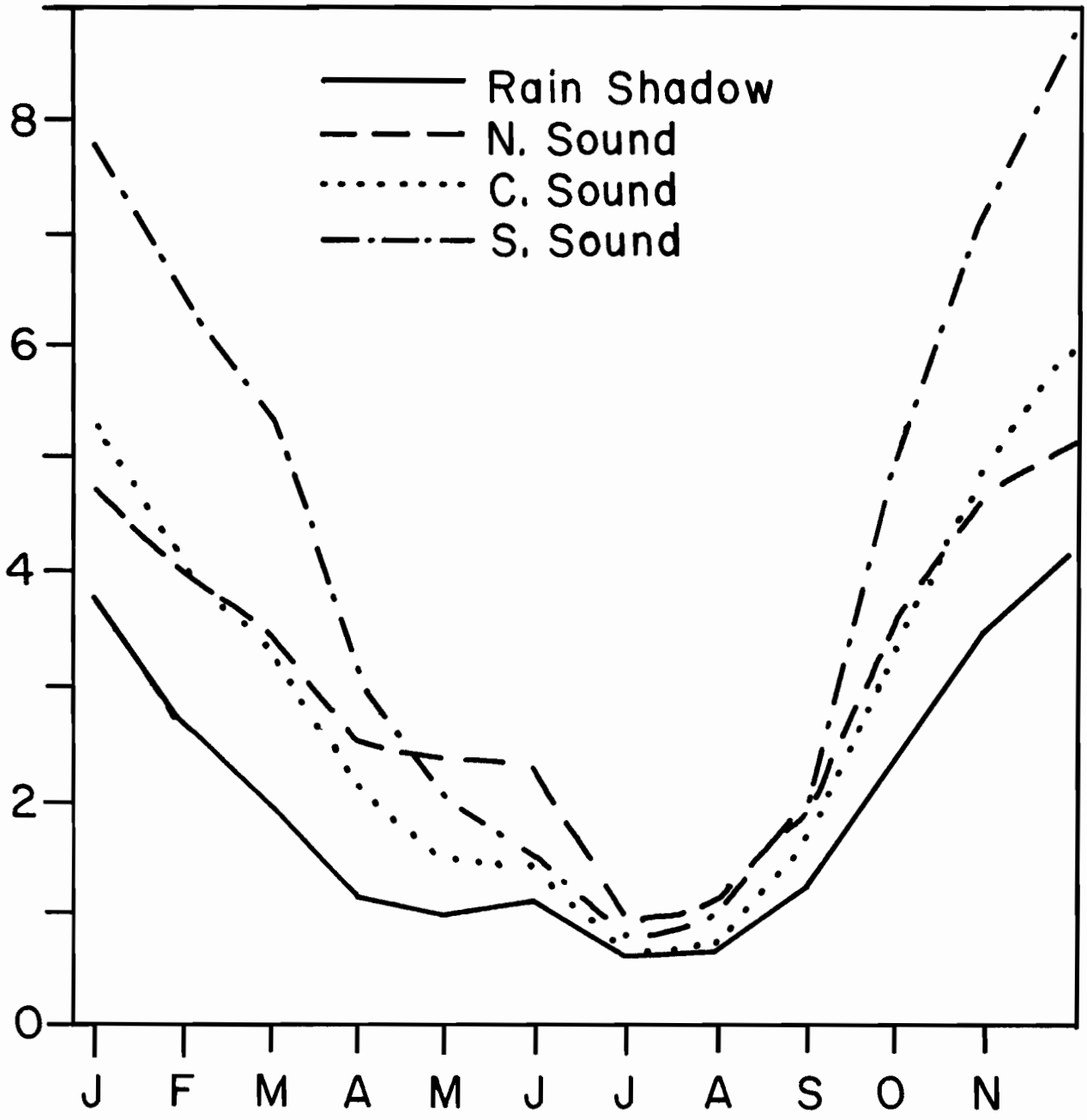

Figure 27. Annual variation of precipitation for the rain shadow and northern, central, and southern Puget Sound regions (Mass, 1981).

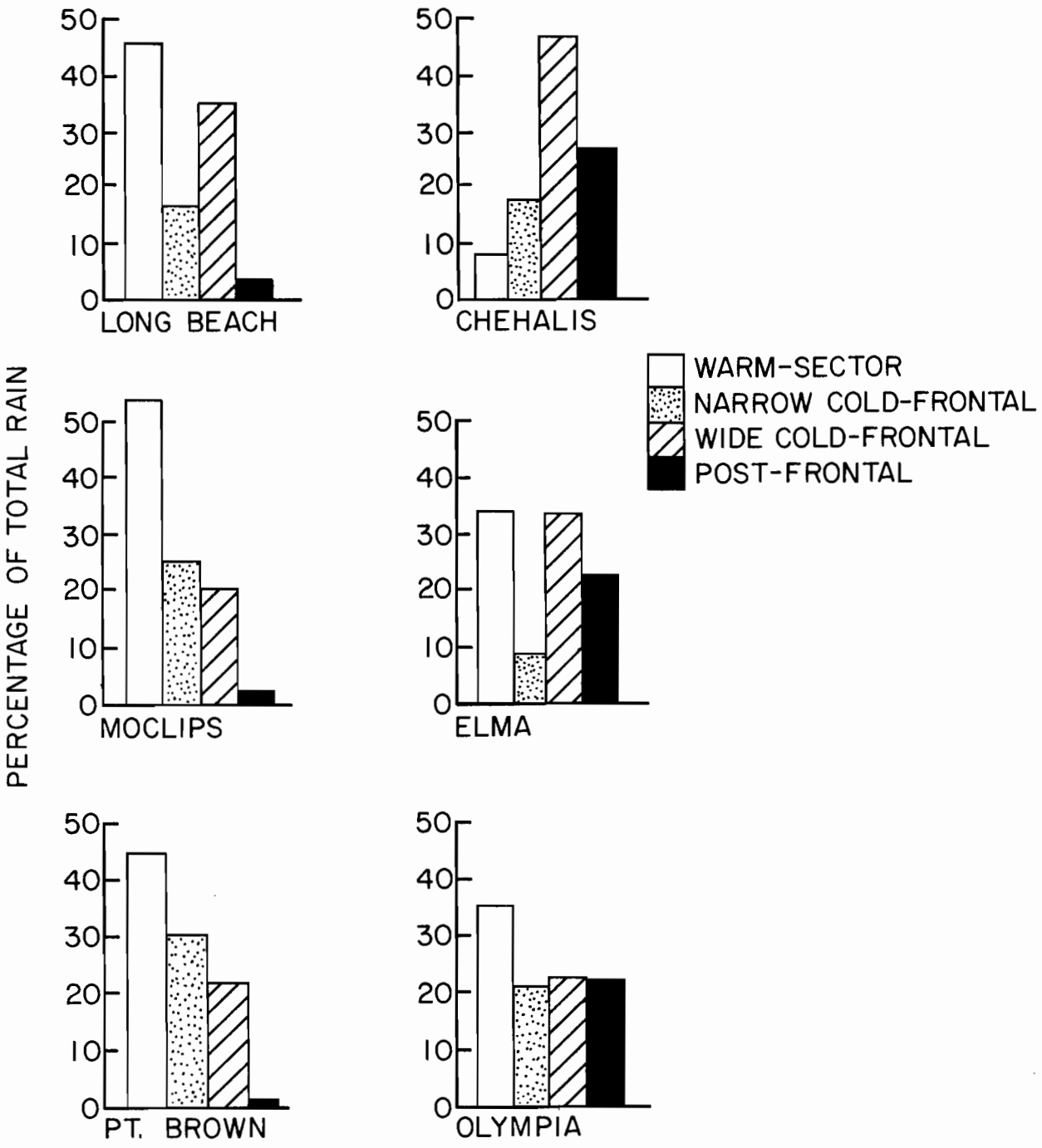

Figure 28. Percentage contributions to total precipitation at three coastal stations (Long Beach, Moclips, Pt. Brown) and three inland stations (Chehalis, Elma, Olympia) from warm sector, narrow cold-frontal, wide cold-frontal, and post-frontal rainbands on 8 December 1976 (Parsons and Hobbs, 1982). Note the large contribution from warm-sector rainbands at the coastal stations and the large contribution from post-frontal rainbands at the inland stations.

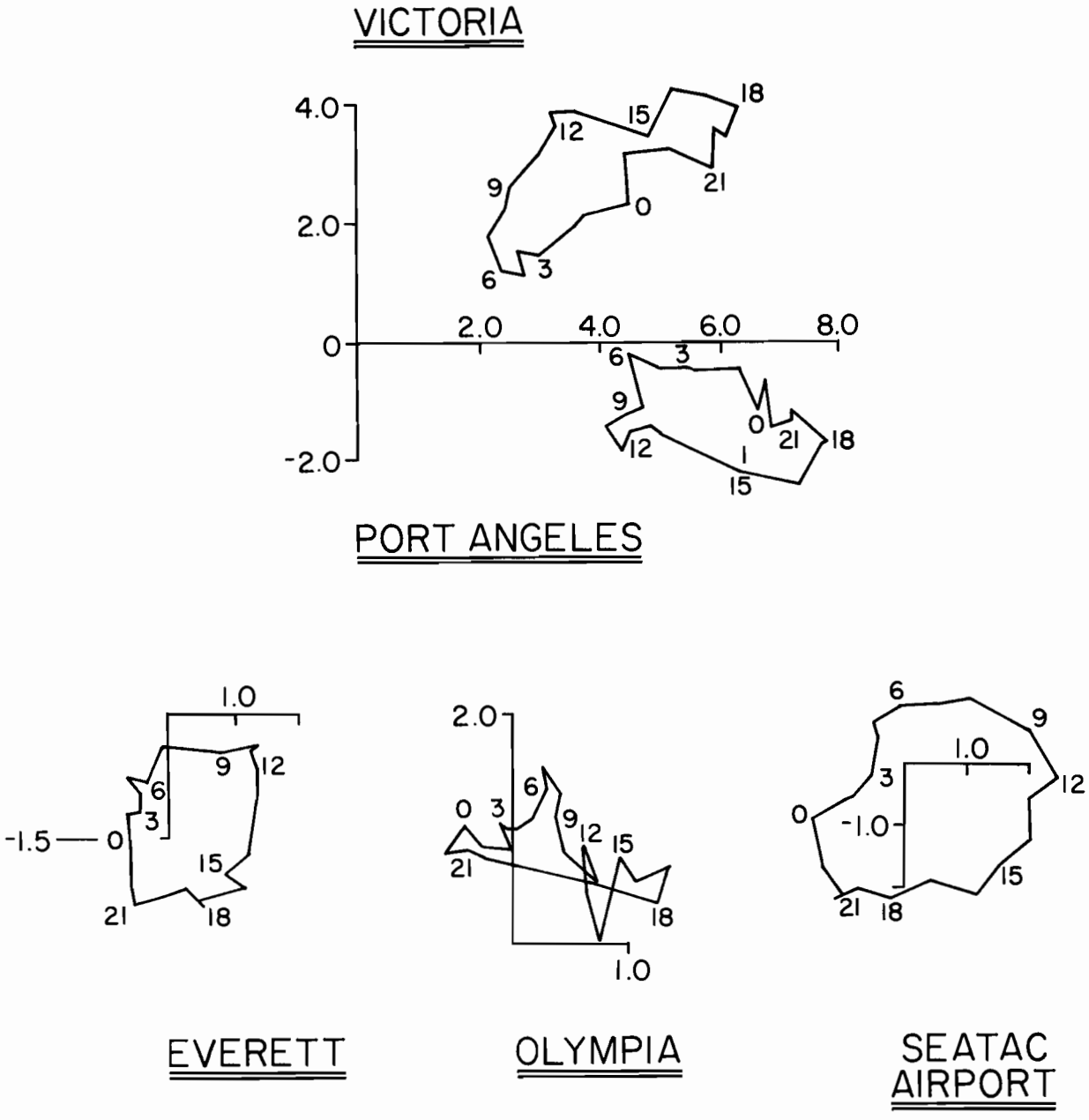

Figure 29. Resultant wind hodographs for stations in the Strait of Juan de Fuca, north, central, and south Puget Sound for July 1950 (Staley, 1957).

6. Acknowledgements

This work is a contribution to the Marine Services Project at the Pacific Marine Environmental Laboratory. We wish to thank Robert Anderson and W. Burton of the NWS Seattle Ocean Services Unit, Don Faulkner, Steve Nikleva, and Ron McLaren of the Canadian Atmospheric Environment Service in Vancouver, B.C., for their support and encouragement of this project.

We wish to thank Drs. Peter Hobbs, Cliff Mass, Richard Reed, Ron Smith, and James Connell for their contributions and suggestions. We also thank *Journal of Fluid Mechanics* (Cambridge University Press) for permission to use figure 21a.

We acknowledge the assistance of Professor Richard Reed, Department of Atmospheric Science, University of Washington, Seattle, Wash. 98195, in providing a copy of an unpublished manuscript by V.F. Morris titled "A study of meso-scale mountain barrier effects in western Washington and Vancouver Island."

7. References

Cannon, G.A. and N.P. Laird (1978): Variability of currents and water properties from year-long observations in a fjord estuary. In: Hydrodynamics of Estuaries and Fjords, Nihoul, J.C.J. ed., Elsevier, Amsterdam, 515-535.

Church, P.E. (1938): Surface details of a warm front in the Strait of Juan de Fuca. Bulletin of the American Meteorological Society, 19, 400-402.

Church, P.E. (1974): Some precipitation characteristics of Seattle. Weatherwise, 27:244-251.

Climatological Handbook, Columbia River Basin States, Hourly Data, Vol. 3, (A and B), (1968): Meteorological Committee, Pacific Northwest River Basin's Commission.

Critchfield, H.J. (1978): Sunshine and solar radiation in Washington State. Office of the State Climatologist, Western Washington University, Bellingham, Washington, 98225, 38 pp.

Drazin, P.G. (1961): On the steady flow of a fluid of variable density past an obstacle. Tellus, 13:239-251.

Faulkner, D.A. (1980): Mesoscale observations of an outflow wind over the Southern Strait of Georgia. Pacific Region Technical Note 80-022, A.E.S., Vancouver, B.C., 6 pp.

Halladay, N.E. (1970): Whidbey Island Forecaster's Handbook, NAV WEA SERV COM INST 3140.2, U.S. Naval Air Station, Oak Harbor, Washington, 115 pp.

Hobbs, P.V., R.A. Houze, Jr., and T.J. Matejka (1975): The dynamical and microphysical structure of an occluded frontal system and its modification by orography. Journal of the Atmospheric Sciences, 32:1542-1562.

Hobbs, P.V. (1978): Organization and structure of clouds and precipitation on the mesoscale and microscale in cyclonic storms. Reviews of Geophysics and Space Physics, 16:741-755.

Hobbs, P.V., T.J. Matejka, P.H. Herzegh, J.D. Locatelli and R.A. Houze, Jr. (1980): The mesoscale and microscale structure and organization of clouds and precipitation in mid-latitude cyclones, I: A case study of a cold front. Journal of the Atmospheric Sciences, 37:568-596.

Hunt, J.C.R. and W.H. Snyder (1980): Experiments on stably and neutrally stratified flow over a model three-dimensional hill. Journal of Fluid Mechanics, 96:671-704.

Klein, W.H. (1957): Principal tracks and mean frequencies of cyclones and anticyclones in the northern hemisphere. Research Paper No. 40, U.S. Weather Bureau, Washington, D.C., 60 pp. (Available from National Weather Service, Techniques Development Laboratory, Washington, D.C. 20233.)

Lau, N.C. (1979): The structure and energetics of transient disturbances in the northern hemisphere wintertime circulation. Journal of the Atmospheric Sciences, 36:982-995.

Locatelli, J.P., P.V. Hobbs and J.A. Werth (1982): Mesoscale structures of vortices in polar air streams. Monthly Weather Review, 110: 1417-1433.

Analysis of the pressure oscillations at several stations (Staley, 1957; Fig. 30) showed a diurnal component that reached its maximum and minimum later at Tatoosh Island on the coast than at the eastern end of the Strait of Juan de Fuca or in Puget Sound. Pressure differences between stations were greatest in the afternoon and early evening driving the westerly sea breeze, but the exact time of maximum pressure difference varied as different pairs of stations were considered. For example, the pressure difference between Port Angeles and Bellingham reached a maximum three to six hours after the maximum pressure difference between Port Angeles and Everett.

Ideally, hodographs should be elliptically shaped, rotate clockwise with time, and fall in strength during the night and increase during the day reaching a maximum between 1330 and 1830 Local Time (LT). Superposition of other factors related to topography, mean flow field, and valley or slope winds upon the sea breeze, however, leads to distortion of this ideal shape and behavior (Mass, 1982); the existence of counterclockwise hodographs must be attributed to topographic constraints. For example, the maximum wind component toward the Cascades during the day and toward Puget Sound at night would be expected on the basis of upslope and drainage winds regardless of sea breeze. In central and northern Puget Sound the winds turn clockwise on the eastern side and counterclockwise on the western side of the Sound. A similar situation exists in the Strait of Juan de Fuca, where Port Angeles on the Olympic Peninsula shows counterclockwise turning while Victoria on Vancouver Island has an oppositely directed hodograph. The figure-eight-shaped hodograph at Olympia is interesting because Olympia is situated at the boundary between two regional sea breeze circulations; it is influenced by the Chehalis Gap to the south and Puget Sound to the north.

5. Summary

The mid-latitude west coast marine climate of the Puget Sound region is typified in summer by a pattern of high pressure and in winter by a sequence of storms that originate over the ocean to the west. Local variations in climatic indicators such as precipitation and wind are substantially influenced by the region's topography. The maximum precipitation occurs in early winter which results in a bimodal distribution of runoff into Puget Sound: there is a winter maximum associated with increased rainfall and a late spring maximum associated with snow melt. The proximity to the Pacific Ocean and the presence of Puget Sound has a moderating influence on extreme temperatures in both summer and winter. Over the waters of Puget Sound the winds near the surface flow from high to low sea-level pressure as imposed by the large-scale or regional weather pattern. Several local wind phenomena are important, the most notable being the formation of an orographically induced, mesoscale low-pressure region in the lee of the Olympic Mountains during strong onshore winds associated with major coastal storms. Such an event produced winds in excess of 50 m s^{-1} in a localized area of Puget Sound at the time of the destruction of the Hood Canal Bridge.

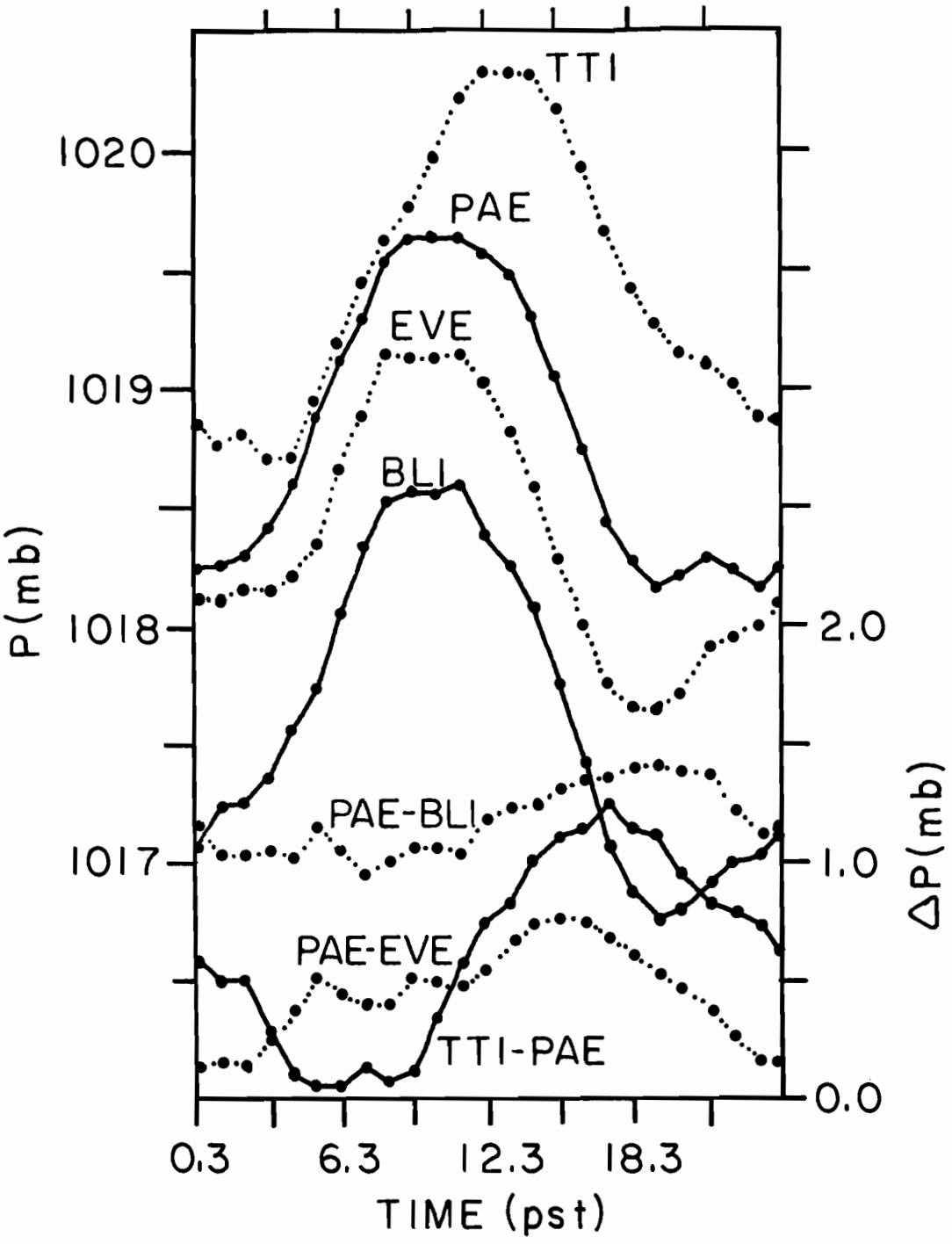

Figure 30. Average sea-level pressures at each hour of the day for July 1950 at Tatoosh Island (TTI), Port Angeles (PAE), Everett (EVE), Bellingham (BLI) (upper four curves); and sea-level pressure differences between Port Angeles and Bellingham, Port Angeles and Everett, and Tatoosh Island and Port Angeles (Staley, 1957).

Lynott, R.E. and O.P. Cramer (1966): Detailed analysis of the 1962 Columbus Day windstorm in Oregon and Washington. Monthly Weather Review, 94:105-117.

Mass, C. (1981): Topographically forced convergence in western Washington state. Monthly Weather Review, 109:1335-1347.

Mass, C. (1982): The topographically forced diurnal circulations of western Washington state and their influence on precipitation. Monthly Weather Review, 110:170-183.

Maunder, W.J. (1968): Synoptic weather patterns in the Pacific Northwest. Northwest Science, 42:80-88.

Mullen, S.L. (1979): An investigation of small synoptic-scale cyclones in polar air streams. Monthly Weather Review, 107:1636-1647.

Myers, R.A. (1966): Lee troughing west of Vancouver Island. CIR-4410, TEC-608, Department of Transport-Meteorological Branch, 5 pp.

National Climatic Center (1980): Local Climatological Data, Annual Summary, Seattle-Tacoma Airport. National Climatic Center, Asheville, N.C., 28801, 4 pp.

Overland, J.E., M.H. Hitchman and Y.J. Han (1979): A Regional Surface Wind Model for Mountainous Coastal Areas. NOAA Technical Report, ERL-407 PMEL-32, Environmental Research Laboratories, National Oceanic and Atmospheric Administration, Boulder, Colorado, 34 pp.

Overland, J.E. (1981): Forecasting the Pacific Northwest winds. Castoff, April 1981, 10-13.

Overland, J.E. and B.A. Walter (1981): Gap winds in the Strait of Juan de Fuca. Monthly Weather Review, 109:2221-2233.

Parsons, D.B. and P.V. Hobbs (1983): The mesoscale and microscale structure and organization of clouds and precipitation in midlatitude cyclones. VIII: Some effects of orography on rainbands. Submitted to Journal of the Atmospheric Sciences.

Phillips, E.L. (1968): Washington climate for these counties, King, Kitsap, Mason, Pierce. Cooperative Extension Service, Washington State University, Pullman, Washington, 66 pp.

Puget Sound Air Pollution Control Agency (1972-1980): Air Quality Data Summary for Counties of King, Kitsap, Pierce, Snohomish. Puget Sound Air Pollution Control Agency, 410 W. Harrison St., Seattle, Washington 98119.

Reed, R.J. (1979): Cyclogenesis in polar airstreams. Monthly Weather Review, 107:38-52.

Reed, R.J. (1980): Destructive winds caused by an orographically induced mesoscale cyclone. Bulletin of the American Meteorological Society, 61: 1346-1355.

Reed, R.J. (1981): A case study of a bora-like windstorm in western Washington. Monthly Weather Review, 109:2383-2393.

Reed, T.R. (1931): Gap winds of the Strait of Juan de Fuca. Monthly Weather Review, 59:373-376.

Reed, T.R. (1932): Weather types of the northeast Pacific Ocean as related to the weather of the north Pacific coast. Monthly Weather Review, 60: 246-252.

Riley, J.J., H.T. Liu, and E.W. Geller (1976): A numerical and experimental study of stably stratified flow around complex terrain. U.S. EPA Environmental Monitoring Series Report No. EPA-600/4-76-021, Research Triangle Park, North Carolina, 30 pp.

Schoenberg, S.A. (1983): Regional wind patterns of the inland waters of western Washington and souther British Columbia. NOAA Technical Memorandum, Environmental Research Laboratories, National Oceanic and Atmospheric Administration, Boulder, Colorado, (in press).

Shore Protection Manual (1973): Vol. 1, U.S. Army Coastal Engineering Research Center, U.S. Government Printing Office, 496 pp.

Skjelbreia, N. (1981): Floating breakwater prototype test program, Department of the Army, Seattle District, Corps of Engineers, (unpublished manuscript).

Smith, R.B. (1980): Linear theory of stratified flow past an isolated mountain. Tellus, 32:348-364.

Smith, R.B. (1981): An alternative explanation for the destruction of the Hood Canal Bridge. Bulletin of the American Meteorological Society, 62: 1319-1320.

Staley, D.O. (1957): The low-level sea breeze of northwest Washington. Journal of Meteorology, 14:458-470.

Walter, B.A. and J.E. Overland (1982): Response of stratified flow in the lee of the Olympic Mountains. Monthly Weather Review, 110: 1458-1473.

Williams, R., H. Pearson, and J. Wilson (1982): Streamflow statistics and drainage-basin characteristics for the Puget Sound Region, Washington. Technical Report, U.S. Geological Survey, Water Resources Division, Tacoma, Washington, in press.